UNIVERSITY of TARTU
Faculty of Mathematics and Computer Science
Institute of Computer Science
Institute of Pure Mathematics

Sergei Šitov

Visualization of Complex Manifolds that are related to Quantum Geometry of Space-time

Master's thesis

Supervisors: Viktor Abramov
Ahto Buldas

TARTU 2007

Index

"'One side will make you grow taller, and the other side will make you grow shorter.'
'One side of what? The other side of what?' thought Alice to herself.
'Of the mushroom', said the Caterpillar."

- Lewis Carroll, Alice's Adventures in Wonderland

1. Introduction

1.1. Road to extra dimensions

Space and time capture the imagination like no other scientific subject. They form the arena of reality – the very fabric of the cosmos. Yet science is still struggling to understand what space and time actually are. Are they real physical entities or just useful ideas?

For thousands of years we thought that space is three-dimensional, that there are up and down, left and right, forth and back. This view arises from our very existence – we are three-dimensional beings and apparently living in three-dimensional space, space that large enough to fit ourselves and whole universe we observe. All our senses are tuned to feel only these three dimensions. Because of that, it almost impossible for us to imagine higher dimensions – forth-dimension, fifth-dimension and so on [1]. However, mathematics could.

Past hundred years we walked long way to understand our space better. We ridded of convenient flat three-dimensional space and submerged to rich mathematical framework that describes curved spaces of any varieties and any sizes. Let's see how that happened and why we think that there are much more extra dimensions than meet the eye [2, 3].

At the beginning of the twenties century, Albert Einstein (1879-1955) overthrew the centuries-old Newtonian framework and gave the world a radically new and deeper understanding of gravitational force. That was a significant leap in our understanding of the universe at whole. But before him, many brilliant scientists strongly contributed to Einstein's success. Foremost among these is the nineteenth-century mathematician Georg Bernhard Riemann $(1826-1866)$ that firmly established the geometrical apparatus for describing curved spaces of arbitrary

dimension. Riemann broke the chains of Euclidean flat-space and paved the way for geometry of all varieties of curved surfaces. It is Riemann's insights that provide the mathematics for describing warped spaces in Einstein's general relativity. Einstein once declared that the mathematics of Riemann's geometry aligns perfectly with the physics of gravity. With general relativity, space-time became a dynamical variable, curving in response to mass and energy. However, theory does not tell us what gravity is or what carriers (bosons) of this force are, it just describes the effects; also, the theory was only good enough to describe universe on large enough scales (celestial bodies, galaxies and tremendously large structures).

One bit of physics that most of pupils have studied in high school is the inverse square law of gravity and electricity. For gravity we have the force between two masses m_1 and m_2 separated by the distance R:

$$G\frac{m_1 m_2}{R^2}$$

(this law was introduced by Isaac Newton; is sufficiently accurate for many practical purposes and is therefore widely used) and likewise, for electricity - the force between two charges separated by distance R:

$$\frac{e_1 e_2}{R^2}$$

That was fine for the first two hundred years, but until electron was discovered. Physicists have had to grapple with the singularity of the inverse square law at $R = 0$ for electricity:

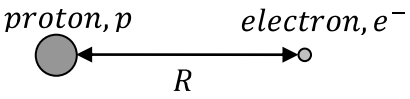

This singularity seemed to imply, for instance, that an atom could survive only about 10^{-9} seconds – electrons orbiting the nucleus would lose their energy through radiation and spiral in towards the nucleus destroying the atom. This demonstrates the complete failure of classical physics when applied to the sub-atomic world. By making use of obvious conclusions drawn from the principles of classical physics, namely the instability of any stationary structure of charged particles and the emission of radiation by a particle moving with acceleration, it is concluded that atoms cannot exist! [4]

This problem, in the case of electricity, was solved with the development of *Quantum Mechanics* at the beginning of twenties century. Developed by Erwin Schrödinger, Werner Heisenberg, Paul Dirac and others, quantum theory was verified to be the correct framework to describe weird world of small constituents of matter and it taught us that the classical notions of the position and velocity of a particle were only approximations of the truth (*Heisenberg's Uncertainty Principle*) – that everything is a bit fuzzy if expressed in classical terms. This principle "smears out" the singularity at $R = 0$. It turns out that quantum uncertainty does not solve the problem for gravity - nonlinear mathematics of general relativity is such that quantum uncertainty alone cannot solve the problem. Fluctuating, jittery picture of space-time predicted by quantum mechanics is in direct conflict with the smooth, orderly geometric model of Einstein's space-time. Nevertheless, quantum mechanics is fantastically accurate. There has never been a prediction of quantum mechanics that has contradicted an observation, so we cannot state that it's wrong. Looks like that for the world of small we need to apply laws of quantum mechanics, but for world of large – general relativity. Logically, laws of nature are supposed to apply everywhere during their symmetrical properties. So, Einstein's laws should apply everywhere and the laws of quantum theory also should apply everywhere, but you cannot have two separate everywheres. We cannot have two configurations of space-time and switch between them, when it suits us.

Meanwhile, physics progressed and, after numerous experiments in particle colliders with hard theoretical work, *Standard Model* of particle physics was created. This is the most successful theory we have that describes world of small constituents of matter and forces. Scientists discovered that there are extra new forces beside electromagnetism and gravity: *weak force*, and *strong force*. These forces are described by, so called, *Yang-Mills gauge theory*.

Weak force is responsible for the process of nuclear beta decay, in which a neutron decays to a proton, an electron, and an antineutrino ($n^0 \rightarrow p^+ + e^- + \bar{\upsilon}_e$). Weak interactions are much weaker than electromagnetic interactions.

Strong force is at play in holding together constituents of the neutron, the proton, the pions, and many other subnuclear particles. These constituents, called quarks, are held so tightly by the strong (or "color") force that they cannot be seen in isolation. The strength of a strong force is increasing with distance.

Since that discovery physics was marked by unifications: events when different phenomena were recognized to be related and theories were adjusted to reflect such recognition.

In the late 1960s the *Weinberg-Salam model* of electroweak interactions put together electromagnetism and the weak force into a unified framework. It was necessary for a predictive and consistent theory of the weak interactions. The theory is initially formulated with four massless particles that carry the forces. But symmetry is breaking and it gives mass to three of these particles: W^+, the W^-, and the Z^0 (carriers of weak force). The particle that remains massless is the photon (carrier of electromagnetic force).

Another type of unification is quantization. Physicists have discovered quantization methods, which can be used to turn a classical theory into a quantum theory – a theory that can be calculated using the principles of quantum mechanics. So all know forces, except gravity, were well quantized and we have *Quantum Electroweak theory* and *Quantum Chromodynamics* (QCD), that describes strong force. These two theories together form the Standard Model.

The Standard Model summarizes completely the present knowledge of particle physics. It tells us that there are three "families" or "generations" of particles that form matter. Each generation has 2 quarks and 2 leptons. First has *up* and *down* quarks, *electron* and *neutrino*. Second - *charm* and *strange* quarks, *muon* and *muon neutrino*. Third - *top* and *bottom* quarks, *tau* and *tau neutrino*. Total 12 matter particles. If we will account such a property that every quark exists in three varieties: quarks have a "*green*", "*red*" or "*blue*" charge, then we will account 24 matter particles. We must not forget negative charges that double number of matter particles – each particle has its antiparticle, so, finally, we end with 48 matter particles. There are also 13 force particles: 8 gluons, 3 weak bosons, photon and graviton (still not directly observed).

Despite the large number of particles, the Standard Model is reasonably elegant and very powerful. However, it has about twenty parameters that cannot be calculated within its framework (for example, mass of the electron) and it does not include gravity. Gravity must be included, with or without unification, if one is to have a complete theory. The effects of the gravitational force are presently quite negligible at the microscopic level, but they are crucial in studies of cosmology of the early universe and

of interior of a black hole, which is incredibly tiny and at the same time incredibly heavy. But, as noted before, Standard Model is quantum theory and Einstein's general relativity is a classical theory (not quantized). It seems very difficult, if not possible, to have a consistent theory that is partly quantum and partly classical.

For decades, every attempt to describe the force of gravity in the same language (with gauge theory) as the other three fundamental forces failed. There were some attempts, which resulted with huge and non-practical gauge group. Later, hint was found and it gave us surprising prediction that our world is not limited to three spatial dimensions.

First attempt for that sort of unification and first idea about existence of extra dimensions of space came in 1919 from German mathematician Theodor Kaluza (1885-1954), who in a few brief pages laid out an approach for unifying gravitational and electromagnetic interactions [5], which, at the time, were the only forces to be well understood. Einstein, who was the referee of Kaluza's paper, did not at first like the idea but eventually warmed to it, accepting it for publication in 1921. Kaluza proposed that the universe is not limited to an only three space dimensions. Instead, he asked physics community to entertain the possibility that the universe has four space dimensions so that, together with time, it has a total of five space-time dimensions. We do not directly observe this extra dimension, so, as proposed later Swedish physicist Oskar Klein, extra dimension must be hiding – curled up in a tiny circle and this circle exist in all points of our usual space-time. In this scheme the electromagnetic field ceased to have any fundamental significance of its own, but was seen merely as component of gravity, albeit in an extra dimension [6]. In other words, electromagnetism is a twists and curves in this fifth dimension.

The Kaluza-Klein idea about extra dimensions was reborn in *String Theory*. String Theory (as one of its features) gives us a quantum-mechanical description of gravity on very short distances near the *Planck length* and is a very good candidate for *Theory of Everything* (TOE*)*. Once one learns to correctly "quantize" the string and compute the "spectrum" – one finds that one of these particles has just the right properties to be the "graviton", or quantum of gravitational waves. This is the beginning of the discovery that in contrast to conventional quantum field theory, which makes gravity "impossible", string theory, actually, requires gravity.

The power of this theory arises from a simple change in thinking – the very basic ingredients of the universe is now not simply infinitely small points, but infinitely thick vibrating strings of energy (in a recent development there are *p*-dimensional membranes or *p*-brains for short). The replacement of particles by strings seems not very important; for the purposes, though, it changes everything. The situation is somewhat analogous to the introduction of Planck's constant $\hbar$ in passing from classical to quantum physics (string theory introduces a new fundamental constant $\alpha' = (10^{-32}\, cm)^2$ controlling the tension of the string). It turns out also that the physical size of strings is set by gravity, more precisely the Planck length $l_p = \sqrt{G_N \hbar c^{-3}} \approx 10^{-33} cm$. This scale is so small that we effectively only see point particles at our distant scales.

Objects now are not of zero dimensions (points), so we need extra degrees of freedom for strings to vibrate and theory states that strings require no more no less but *six* more spatial dimensions. And this is not a trick, literally, theory demands existence of six more dimensions. But what are they?

Since Riemannian geometry is the core of general relativity, this means that it too must be modified in order to reflect the new short-distance physics. String theory asserts that general relativity is true only if we examine the fabric of the universe on large enough scales. However, on scales as small as the Plank length, Einstein's theory suffers from anomalies, that could not be accepted, when we are trying to understand processes inside, for instance, black holes, which are extremely heavy and extremely tiny at the same time. A new kind of geometry must emerge, one that aligns with the new physics of string theory and describe extra dimensions. This new geometrical framework is called *Quantum Geometry.* Simply put, quantum geometry is the appropriate modification of standard classical geometry to make it suitable for describing the physics of string theory.

Unlike the case of Riemannian geometry, there is no ready-to-use mathematical theory for quantum geometry. Instead, physicists and mathematicians are now studying string theory and, step-by-step, piecing together a new branch of physics and mathematics. There is no complete theory yet, but all these investigations have already uncovered many geometrical properties of our space-time (like flop transitions [7]) and gave birth to a completely new level of mathematics.

For instance, there were problems even in quantum field theory and main problem was existence of singularities or infinities. They arise from every nature of particle representation as points and emerge from so called *Feynman diagrams*, which depict particle interactions. The "lines" (or "world-lines" as they called) in a Feynman diagram represent free propagation of particles and the "vertices" are interaction events at which particles branch and rejoin (***Fig. 1.1***). The point of collision is a singularity and moreover diagram produce an infinities when we are trying to calculate, for example, scattering amplitude. That happens, because in calculating a process one must sum over all the possibilities and it leads often to a hard calculation or to infinite result. Sometimes the infinities can be "renormalized" away (what is done for electrodynamics, weak and string interactions).

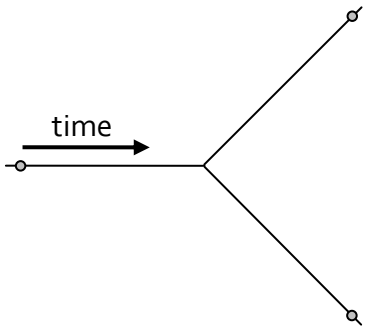

Figure 1.1. ***Feynman diagram of particle interaction***. *Lines represent free propagation of particles and the vertex – interaction point, where particle splits in two. This diagram could represent down quark to up quark decay via the negative weak boson:* $d \rightarrow u + e^{-} + \overline{\nu_e}$.

But, we can apply the same diagrammatic technique with more dimensions in string theory, and then all *world-lines* will become *world-tubes*. Sometimes this is called "pants"-diagram, because of some visual similarity. One consequence of replacing world-lines of particles by world-tubes of string is that Feynman diagrams get smoothed out. World-lines join abruptly at interaction events, but world-tubes join smoothly (***Fig. 1.2***), so no longer an invariant notion of when and where interaction occurs; and we might optimistically hope to have finiteness. These hopes are realized [8-10].

String theory also generates Yang-Mills gauge fields and gauge invariance in close parallel with gravity. Thus, the innocent-sounding operation of replacing world-

lines with world-tubes forces upon us not only gravity but extra degrees of freedom appropriate for unifying gravity with the rest of physical phenomena.

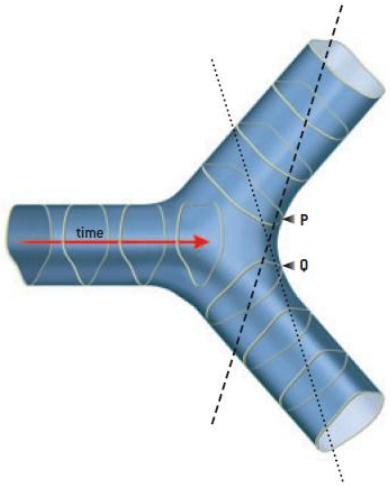

Figure 1.2. ***Feynman diagram of strings interaction.*** *Tubes represent string propagation and diagram has no singular points.*

Still, today we do not have direct experimental data that would confirm existence of extra dimensions, but there is a hope that it would be discovered in new particle colliders (such as *Large Hadron Collider (LHC)* of CERN in Geneva, which will became operational in 2007). For instance, answer could be found by discovery of a *Supersymmetry (SUSY)* phenomenon, which is a hypothetical extension of our understanding of space and time. It includes additional dimensions of space that are "fermionic", and the dimensions themselves actually behave like fermions (matter particles). This means that the new dimensions themselves have weird properties. For example, the photon, which is a boson, when pushed in the direction of a new fermionic dimension becomes a fermion, called "photino", which is boson. Or, a quark, which is fermion, becomes a boson, called a "squark". So, supersymmetry predicts that for every fundamental observed particle in nature (no exceptions, even for graviton) there must exist a corresponding "superpartner". We don't yet see these "superpartners", so if supersymmetry is a valid symmetry, something must be hiding it. Supersymmetry is therefore a broken symmetry. There are other broken symmetries, for example matter and antimatter symmetry, because of it, all matter should have been annihilated in earliest seconds after Big Bang, but it did not happened, so this symmetry is broken (this is also known as *CP-violation*).

Supersymmetry also provides a framework for the unification of particle physics and gravity, which is governed by the Planck energy scale $m_p \approx 10^{19}$ GeV (where the gravitational interactions become comparable in magnitude to the gauge interactions).

Another possibility would be a disappearance of a particle (like graviton) from our space. Since, energy conservation should hold, it would mean that particle shifted somewhere in higher dimension.

1.2. Extra dimensions in string theory

As has been mentioned already, equations of string theory demand existence of six more extra spacial dimensions. We must not forget our usual four dimensional space-time (also called *Minkowski space-time*) $\mathcal{M}^4$ and hence there are ten space-time dimensions at total, so that strings could vibrate in these extra degrees of freedom and produce sufficient amount of quantum properties, which has already been observed in experiments and described by theories. We deal now with objects (strings) that are extended in space and are not infinitely small points, so string theory also sets a lower limit to physically accessible distance scales and proclaims that the universe cannot be squeezed to a size shorter than the Planck length. It is no matter how many points we can pile up on top of each other their combined volume is still zero, but the same we cannot say about strings, if we combine them, they will fill out a nonzero-sized blob, roughly like a Planck-sized ball of entangled rubber bands [1, 2, 7, 11-13].

But of what sizes and shapes these extra dimensions should be? In fact, quantum relativistic superstring cannot propagate in any space-time background. To relate the ten-dimensional string theories (in particular, *heterotic* or *type II* theories[1]) to the four-dimensionality of the world around us, we need to compactify them on a six-dimensional manifold. One possible way of such compactification is simple 6-dimensional torus (would be something similar to Kaluza idea, but much more complex). However, it turns out this would preserve too much supersymmetry. To preserve the minimal amount of supersymmetry, we need to compactify on a special kind of 6-manifold called a *Calabi-Yau manifold* or *Calabi-Yau three-folds* (three here

[1] There are five superstring theories: type I, type IIA, type IIB, $E8 \times E8$ heterotic and $SO(32)$ heterotic. Recently discovered M-Theory unifies all these theories into a one "master theory" through dualities.

refers to three complex dimensions; one can more generally study Calabi-Yau manifolds of arbitrary dimension known as *Calabi-Yau d-folds*) [7, 14]. They are called in honor of two mathematicians, Eugenio Calabi from the University of Pennsylvania (who conjectured it in 1957) and Shing-Tung Yau from Harvard University (who proved it in 1977). If we take the typical radius of such a Calabi-Yau manifold $\mathcal{K}_6^{cy}$ to be small (on the Planck scale) then the ten-dimensional space-time $\mathcal{M}^{10} = \mathcal{M}^4 \times \mathcal{K}_6^{cy}$ will look just like $\mathcal{M}^4$ and hence is consistent with our current observations. String compactification on *Calabi-Yau manifold* leads to supersymmetric four-dimensional vacua. Actually, there are many different Calabi-Yau manifolds and each gives rise to different physics in $\mathcal{M}^4$.

1.3. Computer visualization

Work in the interaction between algebraic geometry and theoretical physics has increased interest in problems involving families of complex algebraic surfaces with some additional structure such as tangent vector bundles. The behavior of these bundles, as singularities develop in the underlying curves, has physical as well as mathematical significance. Visualization methods that increase understanding of these families would be very interesting to mathematicians [15].

Since graphical information is the crucial type for human perception, computer graphics has proven to be a useful tool for researching algebraic manifolds and gaining intuition about them. Generally, visualization helps to uncover some essential properties that are hidden within implicit equations of manifolds, and provides a tool for understanding their geometrical shapes and structures. Theoretically, any manifold described by algebraic equations can be visualized by numerically solving these equations. However, numerical solutions are poorly behaved near singularities and self-intersection. Instead of numerical solutions a method of explicit parametric representation of a manifold's geometry could be applied, which is much simpler and more practical.

In present thesis, these mathematical structures, which are applied in theoretical physics, are described mathematically and visualization methods are applied to render them on computer screen.

2. Theory

2.1. Manifolds

Generally, we will distinguish between three kinds of mathematical structures called *manifolds*, each having increasingly more refined mathematical structure: *topological manifolds*, *differentiable manifolds* and *complex manifolds*. M^n is said to be a n-dimensional topological manifold if it is a *Hausdorff topological space* (any two distinct points can be separated by their neighborhood) locally *homeomorphic* to $\mathbb{K}^n$ (or to some open subset of $\mathbb{K}^n$), where $\mathbb{K}$ is either the field of real numbers $\mathbb{R}$ or the field of complex numbers $\mathbb{C}$. Hence M^n is a n-dimensional topological manifold if for any point $p \in M^n$ there exists an open subset $U \subset M^n$ containing p and homeomorphic (so there exists bijective continuous map and its inverse is also continuous) to $\mathbb{K}^n$. Let us denote by φ a homeomorphism from U to $\mathbb{K}^n$, i.e. $\varphi : U \to \mathbb{K}^n$. Then the pair (U, φ) is called *a local coordinate chart* of a topological manifold M^n (***Fig. 2.1***). If $\varphi(p) = (x_1, x_2, \dots, x_n) \in \mathbb{K}^n$ then the numbers $x_1, x_2, \dots, x_n$ are called the local coordinates of a point p with respect to a local chart (U, φ). An *atlas* of a topological manifold M^n is a set of local charts $\{(U, \varphi)\}_{i \in I}$ such that $\bigcup_{i \in I} U_i = M^n$, i.e. $\{U_i\}_{i \in I}$ is a covering of M^n by open subsets [16].

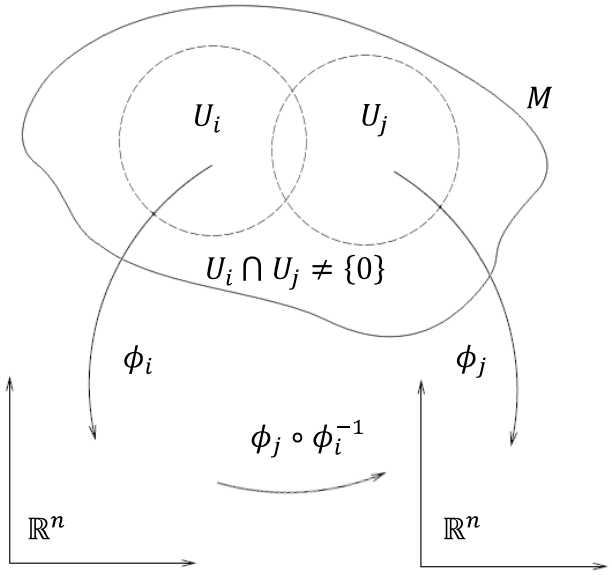

Figure 2.1. ***The charts of a manifold M.***

The topological manifold is called *differentiable manifold* if beside notion of continuity there is a notion of differentiation, so for every non-empty intersections

$U_i \cap U_j$ the transition functions $\phi_j \circ \phi_i^{-1} : \phi_i(U_i \cap U_j) \to \phi_j(U_i \cap U_j)$ are *diffeomorphisms* (they are differentiable and bijective) from $\mathbb{R}^n$ to $\mathbb{R}^n$. By "gluing" all charts together with transition maps an *atlas* of differentiable manifold can be constructed.

Manifold M, with a topology $\mathcal{T}$, is called *compact* if every collection of sets $V_j \in \mathcal{T}$ which covers M (i.e. $M = \bigcup_j V_j$) has a *finite subcover*. For example, the sphere and the n-holed tori are compact manifolds.

The notion of *projective geometry* and *projective space* should be introduced to support description of complex manifolds and altogether it would be a good example of manifolds. This geometry models well the imaging process of a camera because it allows a much larger class of transformations – *perspective projections*. In comparison with *affine geometry*, parallelism is no longer preserved in projective geometry, but these transformations preserve type (points remain points and lines remain lines), incidence (whether a point lies on a line), and a measure known as the *cross ratio* (projective transformations do not preserve neither distances neither ratios of distances, however they preserve ratio of ratios of distances; other words $\frac{d(a,c)d(b,d)}{d(a,d)d(b,c)}$, where $d(p_i, p_j)$ - is Euclidean distance between two points and a, b, c, d are collinear points in projective plane).

Let V^{n+1} be a finite dimensional vector space over the field $\mathbb{K}$, where $\mathbb{K}$ is either the field of real or complex numbers, and v be a nonzero vector of this vector space. It is well known that each nonzero vector v induces the one-dimensional subspace $\mathbb{K}_v$ of V^{n+1}, i.e.

$$\mathbb{K}_v = \{ \lambda \cdot v \ : \ \lambda \in \mathbb{K}, v \neq 0, v \in V^{n+1} \}.$$

The set of all one-dimensional spaces of a vector space V^{n+1} is called the n-dimensional projective space. Let us denote this space by $\mathbb{KP}^n$. Then

$$\mathbb{KP}^n = \{\mathbb{K}_v : v \in \boldsymbol{V^{n+1}}, v \neq \mathbf{0}\}.$$

If $\mathbb{K}$ is the field of real numbers $\mathbb{R}$, then the corresponding projective space is the real projective space $\mathbb{RP}^n$.

Let us define the map $\pi : V^{n+1} \setminus \{0\} \to \mathbb{RP}^n$ by the formula $\pi : v \to \mathbb{R}_v$. Assuming, that a finite-dimensional vector space is equipped with a standard topology, then it is possible to define the topology on the real projective space by saying that a

subset U of $\mathbb{RP}^n$ is open if and only if $\pi^{-1}(U)$ is open in the standard topology of V^{n+1}. Hence, π is a continuous mapping with respect to this topology, it can be proved that $\mathbb{RP}^n$ is topological *Hausdorff space*.

After definition of projective space the notion of *homogeneous coordinates* can be introduced. Homogeneous coordinates have a natural application to computer graphics, especially, to project a complete three-dimensional scene (virtual space) onto a two-dimensional image plane (computer screen). They also unify the treatment of common graphical transformations and operations.

First of all it is necessary to fix a basis $\{e_1, \dots, e_{n+1}\}$ for vector space V^{n+1} and then each vector can be expressed by

$$v = \sum_{i=1}^{n+1} v_i e_i\,, \qquad v_i \in \mathbb{K},$$

where $v_1, v_2, \dots, v_{n+1}$ are coordinates of a vector v with respect to a basis $\{e_1, \dots, e_{n+1}\}$. These coordinates allow us to define the coordinates on the corresponding projective space $\mathbb{KP}^n$ which are called *homogeneous coordinates*. Indeed, if v is a nonzero vector with coordinates $(v_1, v_2, \dots, v_{n+1})$ then the point of the projective space which corresponds to this vector is $\pi(v)$, and we can take the numbers $(v_1, v_2, \dots, v_{n+1})$ as the coordinates of the point $\pi(v)$ of the projective space. However we must take into account that the point $\pi(v)$ of the projective space is the one-dimensional subspace of V^{n+1} generated by v, thus, the coordinates $(w_1, w_2, \dots, w_{n+1})$ of any vector $w = \lambda v$, where $\lambda \neq 0$, of this subspace can be chosen as coordinates of the point $\pi(\vec{v})$. Consequently the homogeneous coordinates $(v_1, v_2, \dots, v_{n+1})$ of the point $\pi(v)$ are defined not uniquely but up to a nonzero factor. Keeping this in mind we shall denote the homogeneous coordinates of a point of projective space by putting the numbers $v_1, v_2, \dots, v_{n+1}$ into square brackets, i.e. $[v_1, v_2, \dots, v_{n+1}]$. Hence we have

$$[\lambda v_1, \lambda v_2, \dots, \lambda v_{n+1}] = [v_1, v_2, \dots, v_{n+1}].$$

Homogeneous points with one zero coordinate called *points at infinity*. In these coordinates, the equation of a line

$$ax_1 + bx_2 + c = 0$$

is given by

$$ax_1 + bx_2 + cx_3 = 0$$

$$u^{\mathrm{T}}p = p^{\mathrm{T}}u = 0$$

where $u = [a, b, c]^{\mathrm{T}}$ is the line and $p = [x_1, x_2, x_3]^{\mathrm{T}}$ is a point on the line, both represented by 3-vectors. This equation can be interpreted as the line u passing through point p, so this symmetry shows that points and the lines have the same representation in the projective plane (*principle of duality*).

By using homogeneous coordinates it is possible to specify differentiable structure and transform real projective space to real differentiable manifold. Let take i-patch

$$U_i = \{[v_1, \dots, v_n] \ : \ v_i \neq 0\} \subset \mathbb{RP}^n, \qquad i = 1, \dots, n.$$

Each U_i is open and projective space itself is a union of all such sets

$$\mathbb{RP}^n = \bigcup_{i=1}^{n} U_i$$

because vector $(v_1, \dots, v_{n+1}) \in V^{n+1} \setminus \{0\}$. We can define continuous map (for a fixed non-negative integer n)

$$h_i : U_i \to \mathbb{R}^n$$

with a continuous inverse map h^{-1}, so

$$h_i([v_1, \dots, v_n]) = \left(\frac{v_1}{v_i}, \dots, \frac{v_{i-1}}{v_i}, \frac{v_{i+1}}{v_i}, \dots, \frac{v_n}{v_i}\right) \in \mathbb{R}^n.$$

This homeomorphism h_i and sets U_i are correctly defined according selection of different homogeneous coordinates. It's also easy to show that $h_i \circ h_j^{-1}$ – *diffeomorphism*, so therefore in $\mathbb{RP}^n$ was specified differentiable structure and it is consistent with definition of differentiable manifold.

Meaning of projective space can be extended with complex numbers - the *n-dimensional complex projective space* $\mathbb{CP}^n$ is the set of all complex lines in $\mathbb{C}^{n+1}$ passing through the origin; as usual origin is excluded from the space, so basically we can define

$$\mathbb{CP}^{\boldsymbol{n}} = \mathbb{C}^{\boldsymbol{n+1}} \backslash \{\boldsymbol{0}\}.$$

The case $n = 1$ gives the complex projective line (can be though of as the complex line $\mathbb{C}$ plus a point at infinity or as the unit (Riemann) sphere in $\mathbb{R}^3$) and the case $n = 2$ - complex projective plane. Basically complex space $\mathbb{C}^n$ has dimension $2n$ over the real's, because it is possible to set complex coordinates with $z_j = x_j + iy_j$ so

$$\mathbb{C}^n \equiv \mathbb{R}^{2n} = \{(x_1, y_1, \dots, x_n, y_n) : \ x_j, y_j \in \mathbb{R}\}.$$

$\mathbb{CP}^n$ is a *complex manifold* of complex dimension n and charts are defined as pairs (U_i, ψ_i) where $\psi_i : U_i \to \mathbb{C}^n$ holomorphic maps, where ψ_i gives a set of complex coordinates $(z_1^i, z_2^i, \dots, z_n^i)$ on U_i. Transition functions $\psi_j \circ \psi_i^{-1} : \psi_i(U_i \cap U_j) \to \psi_j(U_i \cap U_j)$ are also holomorphic as maps from $\mathbb{C}^n$ to $\mathbb{C}^n$. Practically, construction of an atlas of complex manifolds looks almost the same as for manifolds on real numbers.

$\mathbb{CP}^n$ can be described by $n+1$ homogeneous complex coordinates as

$$(z_1, z_2, \dots, z_{n+1}) \in \mathbb{C}^{n+1}, \qquad (z_1, z_2, \dots, z_{n+1}) \neq (0, 0, \dots, 0)$$

with an equivalence relation stating that points labeled by $(z_1, z_1, \dots, z_{n+1})$ are identified with points labeled by $(\lambda z_1, \lambda z_1, \dots, \lambda z_{n+1})$ for any complex number λ. The z_j are therefore not local coordinates in the technical sense. Rather, in the j-th patch, defines by $z_j \neq 0$, we can choose $\lambda = \frac{1}{z_j}$ and use local coordinates

$$([z_1, z_2, \dots, z_n]) = \left(\frac{z_1}{z_j}, \dots, \frac{z_{j-1}}{z_j}, \frac{z_{j+1}}{z_j}, \dots, \frac{z_{n+1}}{z_j}\right).$$

In fact, $\mathbb{CP}^n$ is *compact manifold* and all its submanifolds are compact. There is a famous theorem proved by Chow: a*ny submanifold of* $\mathbb{CP}^n$ *can be realized as the zero locus of a finite number of homogeneous polynomial equations*. An example of this statement is the set of points in $\mathbb{CP}^4$ given by the locus of zeros of the equation $\sum_{i=1}^{5}(z_i)^5 = 0$.

2.2. Tangent spaces

Let M be a real n-dimensional differentiable manifold and $p \in M$ be a point with a local coordinates $p = (p_1, p_2, \dots, p_n)$. Let $\gamma : I \to M$ be a parametrized curve on a manifold M, where $I = (-\epsilon, \epsilon) \subset \mathbb{R}$. Two curves γ_1 and $\gamma_2$are called *tangent* at point $p \in M$, if:

- $\gamma_1(0) = \gamma_2(0) = p$;
- $\frac{dx_i}{dt}(\gamma_1(t))\Big|_{t=0} = \frac{dx_i}{dt}(\gamma_2(t))\Big|_{t=0}$ in some local coordinates $(x_1, x_2, \dots, x_n)$ at a point.

It is easy to show that this definition does not depend on a choice of local coordinates which means that if $\gamma_1$and γ_2 are tangent in one coordinate system, and then they are tangent in any other coordinate system that covers the point $p \in M$. We shall say that two curves γ_1 and γ_2 are equivalent at a point p if they are tangent at this point. It is evident that this is the equivalence relation and we shall denote the class of equivalent curves at a point p induced by a curve γ by $[\gamma]_p$. The vector $\dot{\gamma}_p = \left(\frac{dx_i}{dt}(\gamma_1(t))\Big|_{t=0}\right)$ is called the tangent vector of a curve γ at a point p, and if $[\gamma_1] = [\gamma_2]$ then the equivalence means that these two parametrized curves have the same tangent vector at the point p (***Fig. 2.1***).

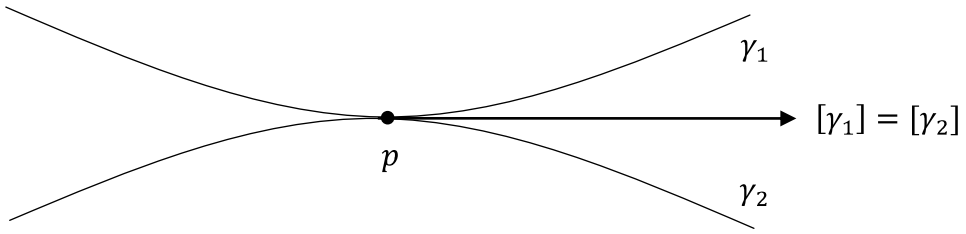

Figure 2.2. ***The equivalence means that these two parametrized curves have the same tangent vector at the point p.***

We may interpret a *tangent vector* at point $p \in M$ as an equivalence class of curves in M where the equivalence relation between two curves is that they are tangent at the point p.

We define the *tangent space* T_pM to a manifold M at a point $p \in M$ as a set of all tangent vectors at the point p. It can be shown that tangent space T_pM is a n-dimensional vector space. It is well known in the theory of smooth manifolds [17] that a tangent vector can be viewed as an operator of differentiation of the algebra of smooth functions of given manifold. In this sense the partial derivative operators

$$T_pM \ : \ \left\{\frac{\partial}{\partial x_1}\Big|_p, \ldots, \frac{\partial}{\partial x_n}\Big|_p\right\},$$

form the holonomic basis for tangent space of manifold M at point p. From this it follows that any tangent vector $v \in T_pM$ can be expressed as $v = v_i \frac{\partial}{\partial x_i}\Big|_p$. This expression directly captures what tangent vector really is: a first order motion along M.

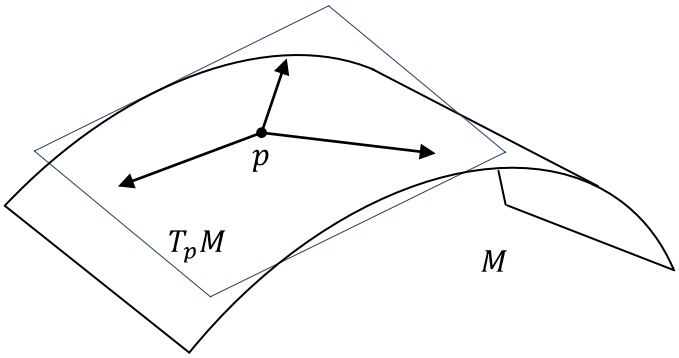

Figure 2.3. ***The tangent space and tangent vectors on M at point p.***

The *tangent bundle* TM of a manifold M is defined as

$$TM = \bigcup_{p \in M} T_pM \,.$$

The *cotangent space* T_p^*M is the vector space that is dual to T_pM. The dual basis for holonomic basis is the basis

$$T_p^*M : \left\{ dx_1|_p, \dots, dx_n|_p \right\},$$

where $dx_i : T_pM \to \mathbb{R}$ is 1-forms or linear maps defined by $dx_i\left(\frac{\partial}{\partial x_j}\right)\Big|_p = \delta_j^i$. The dx_i are called linear 1-forms.

If M is a complex manifold, there is a notion of the complexified tangent space of M, $T_pM^{\mathbb{C}}$, this space is the same as the real tangent space T_pM except that complex coefficients are allowed to be used in the vector space manipulations. In terms of complex coordinates it is possible to write a basis of tangent space with holomorphic and anti-holomorphic directions:

$$T_pM^{\mathbb{C}} : \left\{ \frac{\partial}{\partial z_1}\Big|_p, \dots, \frac{\partial}{\partial z_d}\Big|_p, \frac{\partial}{\partial \bar{z}_1}\Big|_p, \dots, \frac{\partial}{\partial \bar{z}_d}\Big|_p \right\}$$

where $d = n/2$ is a complex dimension and

$$\frac{\partial}{\partial z_i}\Big|_p = \left(\frac{\partial}{\partial x_i} + i\frac{\partial}{\partial x_{d+i}}\right)\Big|_p \quad , \quad \frac{\partial}{\partial \bar{z}_i}\Big|_p = \left(\frac{\partial}{\partial x_i} - i\frac{\partial}{\partial x_{d+i}}\right)\Big|_p \,.$$

The same goes for dual space

$$T_p^*M^{\mathbb{C}} : \left\{ dz_1|_p, \dots, dz_d|_p, d\bar{z}_1|_p, \dots, d\bar{z}_d|_p \right\}.$$

2.3. Metrics

The *metric* is a positive definite inner product on T_pM which smoothly depends on a point p, or in other words it is a symmetric bilinear positive definite map

$$g : T_pM \times T_pM \to \mathbb{R}.$$

Given two vectors v and v' in T_pM let us denote their inner product as $g(v, v')$. Since a metric is bilinear in its arguments, the value of this metric on any two vectors can be expressed in terms of its values on basis elements

$$g\left(\frac{\partial}{\partial x_j}, \frac{\partial}{\partial x_k}\right) = g_{jk},$$

where g_{jk} are called the metric coefficients in holonomic basis. Thus,

$$g(v, v') = g\left(v_j \frac{\partial}{\partial x_j}, v'_k \frac{\partial}{\partial x_k}\right) = g_{jk} v_j v'_k ,$$

and metric can be written as

$$g = g_{jk} dx_j \otimes dx_k,$$

where the metric coefficients satisfy the symmetric relation $g_{jk} = g_{kj}$. If we have a metric g on a manifold we define the length of a tangent vector v by the formula $|v|^2 = g(v, v)$. This shows that metric allows us to measure lengths of tangent vectors with respect to metric $g(v, v')$ and we can measure distances on M by introducing with the help of a metric a notion of geodesic curves [17, 18].

If M is a complex manifold, there is a natural extension of the metric g to a map

$$g : T_pM^{\mathbb{C}} \times T_pM^{\mathbb{C}} \to \mathbb{C} .$$

Let r, s, v, w be vectors in T_pM. Using these vectors it is possible to construct two complex vectors $z = r + is$ and $z' = v + iw$ which lie in $T_pM^{\mathbb{C}}$. Then metric g can be evaluated by linearity:

$$g(z, z') = g(r + is, v + iw) = g(r, v) - g(s, w) + i(g(r, w) + g(s, v)).$$

The original metric can be extended then with respect to complex coordinates by the formulae $g_{jk} = g\left(\frac{\partial}{\partial z_j}, \frac{\partial}{\partial z_k}\right)$, $g_{j\bar{k}} = g\left(\frac{\partial}{\partial z_j}, \frac{\partial}{\partial \bar{z}_{\bar{k}}}\right)$ and so on. The symmetry of original metric implies that in a complex coordinates $g_{jk} = g_{kj}$, $g_{j\bar{k}} = g_{\bar{k}j}$ and $\overline{g_{jk}} = g_{\overline{kj}}$, $\overline{g_{j\bar{k}}} = g_{k\bar{j}}$.

2.4. Hermitian and Kähler manifolds

Let us consider a holomorphic complex function $f(z)$ of one variable $z = x + iy$. Let us write $\bar{z} = x - iy$ as the *complex conjugate* of z. Now we have two pairs of variables: $\{x, y\}$ and $\{z, \bar{z}\}$, which are related by

$$z = x + iy, \quad \bar{z} = x - iy, \quad x = \frac{z + \bar{z}}{2}, \quad y = \frac{z - \bar{z}}{2i}.$$

These relations can be formally carried over to differentials:

$$dz = dx + idy, \quad d\bar{z} = dx - idy, \quad dx = \frac{dz + d\bar{z}}{2}, \quad dy = \frac{dz - d\bar{z}}{2i}.$$

Let M be a n-dimensional complex manifold. Let $(z_1, z_1, \dots, z_n)$ be a local complex coordinates on n-dimensional complex manifold. Let TM be a complex tangent bundle and T^*M be a dual complex cotangent bundle of complex manifold M. T_pM is a $2n$-dimensional vector space over the real numbers. Using previously defined notations we can write $z_k = x_k + iy_k$, where x_k, y_k are local real coordinates, and dx_k, dy_k form a basis for T_p^*M, and $\frac{\partial}{\partial x_k}, \frac{\partial}{\partial y_k}$ form basis for T_pM. Let

$$dz_k = dx_k + idy_k$$
$$d\bar{z}_k = dx_k - idy_k.$$

Since dx_k, dy_k form a basis of T_p^*M, then dz_k, $d\bar{z}_k$ form a basis of complex linear forms for $T_pM^{\mathbb{C}}$.

In local complex coordinates, a metric g is called *Hermitian* if $g_{jk} = g_{\overline{jk}} = 0$. In such a case, only the mixed type components (like $g_{j\bar{k}}$, $g_{\bar{k}j}$) of metric g are nonzero and it can be written as

$$g = g_{j\bar{k}} dz_j \otimes d\bar{z}_{\bar{k}} + g_{\bar{j}k} d\bar{z}_{\bar{j}} \otimes dz_k .$$

Hermiticity is a restriction on the metric and not on the manifold. A complex manifold M is called *Hermitian manifold* if it is endowed with a Hermitian metric.

We remind that a wedge product of two 1-forms is defined as follows

$$dz_A \wedge dz_B = dz_A \otimes dz_B - dz_B \otimes dz_A = -dz_B \wedge dz_A,$$

where $A, B = \{(j,k), (j,\bar{k}), (\bar{j},k), (\bar{j},\bar{k})\}$. Given a Hermitian metric g on manifold M we define the $(1,1)$-form in the space of $(1,1)$-forms $\Omega^{1,1}(\mathrm{M})$ by the formula

$$\omega = ig_{j\bar{k}} dz_j \otimes d\bar{z}_{\bar{k}} - ig_{\bar{j}k} d\bar{z}_{\bar{j}} \otimes dz_k .$$

Making use of the symmetry $g_{j\bar{k}} = g_{\bar{k}j}$ and the *wedge product* we can express the above form as

$$\omega = ig_{j\bar{k}} dz_j \wedge d\bar{z}_k \,.$$

A form θ is called a closed form if its exterior differential equals to zero, i.e. $d\theta = 0$. Then ω is called a *Kähler form* if it is closed and manifold M is called a *Kähler manifold*.

Simplest example of the Kähler manifold is $\mathbb{C}^n$. For this manifold a Kähler form associated to the usual Euclidean metric written in a complex coordinates

$$g = \sum_j dz_j \otimes d\bar{z}_j$$

as

$$\omega = \frac{i}{2} \sum_j dz_j \wedge d\bar{z}_j \,.$$

Form ω, in this example, is closed and it is easy to show it:

$$d\omega = d\left(\frac{i}{2} \sum_j dz_j \wedge d\bar{z}_j\right) = \frac{i}{2} \sum_j (d^2 z_j \wedge d\bar{z}_j - dz_j \wedge d^2 \bar{z}_j) = 0,$$

because of the following properties of forms

$$d^2\theta = 0,$$

$$d(\theta_1 \wedge \theta_2) = d\theta_1 \wedge \theta_2 + (-1)^p \theta_1 \wedge d\theta_2,$$

where θ_1 is a p-form.

The ordinary complex projective space $\mathbb{CP}^n$ is also Kähler.

2.5. Holonomy

Let M be a real n-dimensional differentiable manifold and let $v \in T_p M$. Assuming that M is equipped with a metric g and the associated connection Γ (also called *Levi-Civita connection*), we can imagine parallel transporting v along a closed curve γ in M, which begins and ends at p. After the journey around the curve, the vector v will generally not return to its original orientation in $T_p M$. Then v will return to p pointing in some another direction v' (length of vector will be unchanged), except, if M is flat. If M is orientable, the vectors v and v' will be related by a $SO(n)$[2] transformation A_γ. That is

$$v = A_\gamma v'.$$

[2] *Special Orthogonal Group*. For example, the group $SO(3)$ is understood as the set of rotations in 3-dimensional space.

If we consider all possible closed curves $(\gamma_1, \gamma_2, \dots)$ in M which pass through p, and repeat the above procedure, this will yield a collection of $SO(n)$ matrices $A_{\gamma_1}, A_{\gamma_2}, \dots$, one for each curve. So, if we traverse a curve γ which is the curve γ_i followed by the curve γ_j, then associated matrix will be $A_{\gamma_i} A_{\gamma_j}$. If we traverse the curve γ_i in reverse, the associated matrix will be $A_{\gamma_i}^{-1}$. Thus, the collection of matrices generated in such manner form a group – some subgroup of $SO(n)$. Lets follow the same procedure for all points p on M. The similar reasoning ensures that new collection of matrices also forms a group. This group describing how vectors change upon parallel translating around loops on M is called the *holonomy* of M [7].

If M is Kähler manifold then, by using certain simplifications which occur in the Kähler differential geometry associated to M, the holonomy matrices can be consistently written in terms of their action on the holomorphic or anti-holomorphic basis elements and hence lie in a $U(n/2)$ subgroup[3] of $SO(n)$. There are special cases of Kähler manifolds whose holonomy group is even further restricted to lie in $SU(n/2)$ [4] [7].

2.6. Calabi-Yau manifolds

An n-dimensional manifold is known as *Calabi-Yau manifold* if it satisfies the following properties:

- it is compact,
- it is complex,
- it is Kähler,
- it has $SU(n/2)$ holonomy.

In one complex dimensions (*one-fold*), the only Calabi-Yau manifolds are family of *tori*. In two complex dimensions (*two-fold*) - $K3$ *manifolds*. Perhaps the simplest and certainly the most popular Calabi-Yau manifold of complex dimension 3 (*three-fold*) is the *quintic hypersurface* (an algebraic surface of degree five) in complex projective four-

[3] *Unitary Group. The matrix A is unitary if $A\bar{A}^T = E$.*
[4] *Special Unitary Group*. The matrix A is special unitary if it is unitary and $|A| = 1$.

space $\mathbb{CP}^4$ with homogeneous coordinates $(z_1, \dots, z_5)$ given by the locus P [7], i.e., the space of solutions to a *quintic holomorphic constraint* in $\mathbb{CP}^4$:

$$\boldsymbol{P(z_1, \dots, z_5) = \sum_{i=1}^{5} (z_i)^5 = 0}$$

or simply

$$\boldsymbol{z_1^5 + z_2^5 + z_3^5 + z_4^5 + z_5^5 = 0.}$$

This hypersurface is non-singular and moreover it is a Kähler manifold, inheriting this property from the complex projectional space $\mathbb{CP}^4$. Thus, of course, the manifold itself has dimension $(n-1)$, which is 3 complex dimensions or 6 real dimensions. The families of such hypersurfaces are usually denoted by 'bra-ket' notation $\mathbb{P}[4\|5]$, where the left-most, 'bra' entry is the dimension of $\mathbb{CP}^n$ and remaining, 'ket' entries are the degrees of homogeneity of the polynomials.

In the beginning, there were following Calabi-Yau manifolds:

- The quintic in $\mathbb{CP}^4$, denoted as $\mathbb{P}[4\|5]$;
- The intersection of two cubics in $\mathbb{CP}^5$, denoted as $\mathbb{P}[5\|3\ 3]$;
- The intersection of a quadric and a quartic in $\mathbb{CP}^5$, denoted as $\mathbb{P}[5\|2\ 4]$;
- The intersection of two quadrics and a cubic in $\mathbb{CP}^6$, denoted as $\mathbb{P}[6\|2\ 2\ 3]$;
- The intersection of four quadrics in $\mathbb{CP}^7$, denoted as $\mathbb{P}[7\|2\ 2\ 2\ 2]$;

Soon after followed complete intersections of polynomial hypersurfaces in direct products of projective spaces, and then transverse polynomials in *weighted projective spaces*. Most recently Calabi-Yau manifolds have been constructed as embeddings in toric varieties [19].

2.7. Kummer and $K3$ surfaces

Consider a family of *quartic* (algebraic surface of degree four) hypersurfaces [20]

$$X_\lambda : (\lambda(x^4 + y^4 + z^4 + w^4) = (x^2 + y^2 + z^2 + w^2)^2) \subset \mathbb{CP}^3.$$

For general λ, the surface X_λ is nonsingular. In fact, this family is singular at $\lambda = 1, 2, 3, 4$, and at $\lambda = 0$ where the surface is seen to be a *double quadric*.

Let fix $w = 1$ and $\lambda = 2$, then

$$\lambda(x^4 + y^4 + z^4 + 1) = (x^2 + y^2 + z^2 + 1)^2$$

$$\lambda(x^4 + y^4 + z^4 + 1) -$$
$$-(x^4 + y^4 + z^4 + 2x^2 + 2y^2 + 2z^2 + 2x^2y^2 + 2x^2z^2 + 2y^2z^2 + 1) = 0$$
$$(x^4 + y^4 + z^4) - 2(x^2 + y^2 + z^2) - 2(x^2y^2 + x^2z^2 + y^2z^2) = 0.$$

So, finally, an implicit equation can be derived and the surface is a set of points (x, y, z) satisfying the equation

$$x^4 + y^4 + z^4 - x^2 - y^2 - z^2 - x^2y^2 - x^2z^2 - y^2z^2 - 1 = \varpi$$

and can be easily visualized with different ϖ parameters by Marching Cubes algorithm (***Fig. 4.5, 4.6, 4.7***).

When $\varpi = 0$ then equation above describes *Kummer* surface (***Fig. 4.5***) - the surface what is known as quartic Calabi-Yau surface in the complex three dimensional projective space with 16 double points (or singularities), the maximum possible for a surface of degree four in three-dimensional space. The symmetry is corresponding to the cube hidden in the central part and clearly visible on the plot. However, it is very difficult to foresee such symmetry only from defining equation.

A non-singular quartic surface ($\varpi > 0$) in projective space of three complex dimensions is a $K3$ surface (***Fig. 4.6***). The $K3$ surface is the standard playground for testing many ideas in string theory for many years. For instance, in *M-Theory* (latest "master theory" that unifies the five superstring theories) compactifications can be done on $K3 \times K3$ [21, 22].

Kummer surfaces can also be described by using tetrahedral coordinates as algebraic equation (more common definition)

$$X_{4,\mu} = (x^2 + y^2 + z^2 - \mu^2\varpi^2)^2 - \lambda pqrs = 0$$
$$\lambda = \frac{3\mu^2 - 1}{3 - \mu^2}, \ \ \mu \in \mathbb{R}$$
$$p = \varpi - z - \sqrt{2}x$$
$$q = \varpi - z + \sqrt{2}x$$
$$r = \varpi + z + \sqrt{2}y$$
$$s = \varpi + z - \sqrt{2}y$$

where μ is a deformation parameter, ϖ is a scaling parameter (usually set to 1) and p, q, r, s are tetrahedral coordinates (***Fig. 4.1, 4.2, 4.3, 4.4***) [23]. On plot with deformation parameter $\mu = \sqrt{2}$, 16 double points are clearly visible (***Fig. 4.2***). Animation may also be constructed by varying deformation parameter μ.

3. Visualization

3.1. Methods

There are two different ways to visualize a manifold. When manifold described as algebraic equation of the form

$$\boldsymbol{f(x_1, .., x_n) = \sum_n c_{e_1,\dots,e_n} x_1^{e_1} \dots x_n^{e_n} = k}$$

(where the coefficients $c_{e_1,\dots,e_n}$ are integers, the exponents e_i are nonnegative integers and the sum is finite) then it is possible to visualize it by numerically solving the equation and by generation of a lattice of simplices by *Marching Cubes* algorithm. When manifold is described parametrically of the form

$$\boldsymbol{\alpha(t_1, \dots, t_n) = \begin{cases} x_1 = f_1(t_1, \dots, t_n) \\ \dots \\ x_n = f_n(t_1, \dots, t_n) \end{cases}}$$

(where $t_1, \dots, t_n$ are independent parameters) then a *Parametric Plot* yields a visual description of a set of manifold's parametric equations.

First method requires a lot of computational power and memory (especially for higher dimensions). Second method is usually very simple and fast, so calculations can be done in real-time with relatively less powerful computer. Exact parametric representation of a manifold shall be known in this case, however the disadvantage is that not all manifolds can be described parametrically or derivation of parametric form can be very complicated.

In present thesis both methods are described, implemented and used to produce plots.

3.2. Marching cubes

Isosurface visualization is very important within scientific visualization. The *isosurfaces* depict a value of equal density or display the surrounds of specified objects within the scalar data. Likewise, in two dimensions, we can use contour plots to display the information, thus, similarly, in three dimensions surfaces may be formed around objects and in four dimensions hypersurfaces around hyperobjects [24].

On $3D$ plots these isosurfaces are often formed from a set of connected triangles. These piecewise segments represent the simplest non-degenerate object of that dimension and are named *simplices*. Triangle is a 2-simplex, a tetrahedron is a 3-simplex and a "hypertetrahedron" is a 4-simplex, and so on (***Fig. 3.1***).

$1D$		*Point*, (0-polytope or 0-simplex)
$2D$		*Line*, 1 edge, (1-polytope or 1-*simplex*)
$3D$	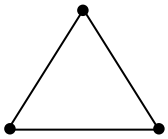	*Triangle*, 3 edges, (2-polytope or 2-*simplex*)
$4D$	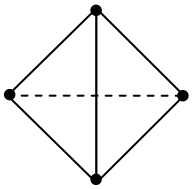	*Tetrahedron*, 6 edges, (3-polytope or 3-*simplex*)
$5D$	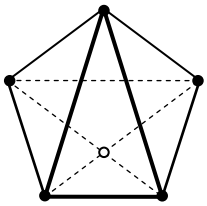	*Hypertetrahedron* or *Pentachoron*, 10 edges, (4-polytope or 4-*simplex*)

Figure 3.1. ***Simplices for different dimensions.***

Thus, a continuous n-dimensional surface may be represented by a lattice of connected $(n-1)$-dimensional simplices. This lattice of connected simplices can be calculated over a set of adjacent n-dimensional hypercubes, via the *Marching Cubes algorithm* [24-28].

This algorithm uses a divide-and-conquer approach to locate an isosurface defined by some algebraic equation in a n-dimensional grid. Algorithm samples the equation on each vertex for single grid's cell (square, cube, hypercube, …) and then moves (or "marchs") to the next cell and so on. If the value at some vertex exceeds (or equals) the value of the surface (isovalue) then algorithm consider this vertex inside (or

on) the surface (on pictures, points that are inside the surface are full). Vertices with values below the surface are considered outside the surface. With this assumption, it is possible to define a topology of the surface within a cell by finding the locations of the intersections (***Fig. 3.2***).

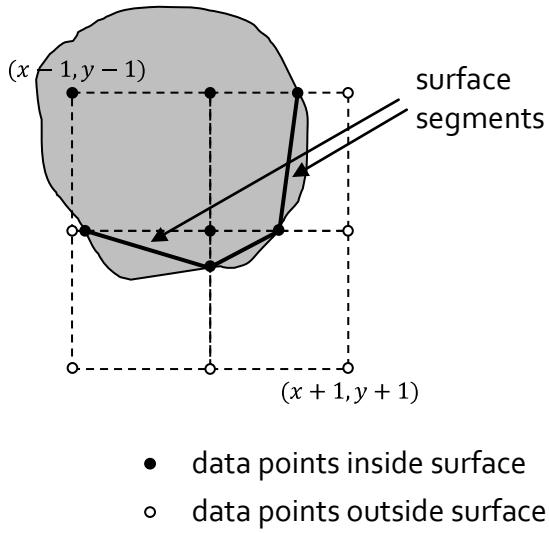

Figure 3.2. ***Vertices with values that exceed (or equal) the isovalue are inside the surface and vertices that are below are outside.*** *By these points it is possible to interpolate surface segments.*

Basically, the Marching Cubes algorithm can be divided into two primary steps. First, it generates the *lookup table* for a given dimension n. Secondly, using this lookup table, it contours the regular n-dimensional grid by locating the n-hypercubes which are intersected by the isosurface. The lookup table algorithm creates an index for each possible isosurface-edge intersection with a hypercube, based on the state of the vertex (an edge of the n-hypercube intersects the isosurface if one endpoint has a positive isovalue and one endpoint has a negative isovalue). The table contains the edges interested for each intersection case. So, for instance, if isosurface intersected some vertices then algorithm can easily determine all edge intersections by looking to this index, which will return a set of edges. By using this set of edges from the index algorithm can interpolate the real isosurface intersections along the edges (present implementation uses simple linear interpolation). Theoretically, isosurface lookup tables can be constructed for any dimension; however, for example, a five dimensional hypercube has $V = 32$ vertices and, thus, $L = 2^{32} = 4\,294\,967\,296$ possible intersections. For this, huge amount of computer memory would be required to simply

store the index (index key will be 4 bytes of size and to store edges - from 0 to 32 bytes are required, so at total several dozens of gigabytes). In the case of higher dimensions it is possible not to construct a lookup table, but to directly generate the isosurface patches in each n-hypercube. However, this would take much longer time than with lookup table.

Generally, the algorithm executes the following steps to calculate an isosurface of some algebraic equation:

1. Algorithm divides a n-dimensional volume into a regular grid of n-dimensional hypercubes (***Fig. 3.3***). The edges of the grid are the edges of these hypercubes.

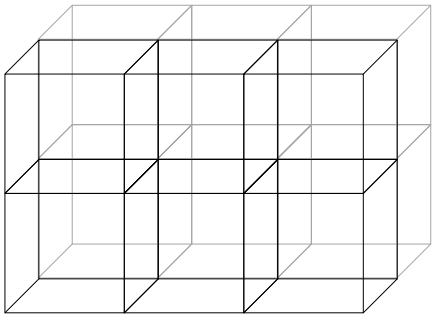

Figure 3.3. ***3-dimensional grid of cubes for 3-dimensional space.***

2. Algorithm enumerates vertices and edges of a single n-dimensional hypercube. Each vertex has a coordinate (just relative location from $(0, 0, \dots)$) and its index number (***Fig. 3.4***). Each edge described by two numbers – the number of first vertex and the number of last vertex; and by an order number.

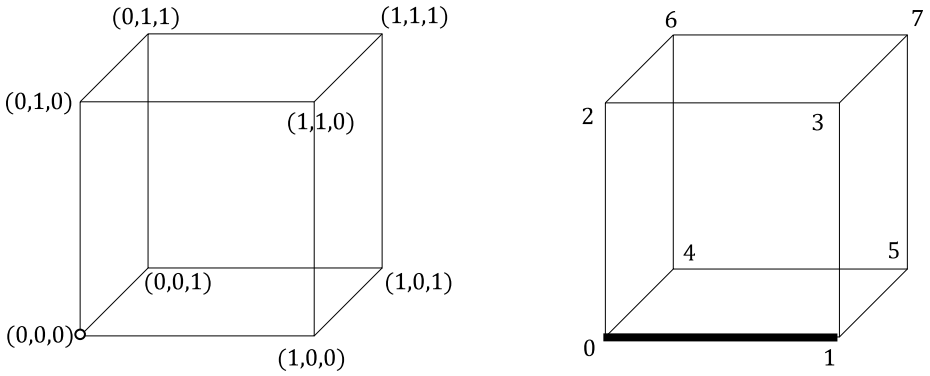

Figure 3.4. ***Enumeration of vertices and edges for a 3-dimensions.***

Algorithm uses edge numbers them to calculate facets and for other purposes. Edges are sorted in lexicographical order:

$$(0,1;0), (0,2;1), (1,3;2), (2,3;3), (0,4;4), (1,5;5), (2,6;6), (3,7;7),$$
$$(4,5;8), (4,6;9), (5,7;10), (6,7;11)$$

The number of vertices can be calculated by $V = 2^n$ and the number of edges by $E = \frac{Vn}{2}$, so for 3-dimensions $V = 8$ and $E = 12$ (which is obvious), and for 4-dimensions $V = 16$ and $E = 32$.

3. Algorithm enumerates all facets ("sides") of a n-dimensional hypercube into a binary code. The number of facets can be calculated by $F = 2n$ (a 1-dimensional line has 2 points ("sides"), a 2-dimensional square has 4 sides, a 3-dimensional cube has 6 2-dimensional facets, a 4-dimensional hypercube has 8 3-dimensional cells). Because cube has 8 vertices so for 3-dimensions code can fit into one byte:

Facet	Binary code
(0,2,4,6)	01010101
(1,3,7,5)	10101010
(0,1,4,5)	00110011
(2,3,6,7)	11001100
(0,1,2,3)	00001111
(4,5,6,7)	11110000

For 4-dimensons code can fit into unsigned long type (4 bytes). Binary code used further to determine - is selected edge located on a specific facet or not.

4. Algorithm generates a lookup table. Because, there are 2^n vertices of a n-dimensional hypercube, there are 2^{2^n} ways how isosurface can intersect the hypercube and so 2^{2^n} different vertex labelings at total. Thus, the size of a lookup table can be calculated by $L = 2^{2^n}$. For 2-dimensions $L = 2^4 = 16$ (***Fig. 3.5***), for 3-dimensions $L = 2^8 = 256$ and for 4-dimensions $L = 2^{16} = 65536$ entries [25]. The single table entry has a key code of a single vertex labeling and a set of intersected edges of a n-hypercube.

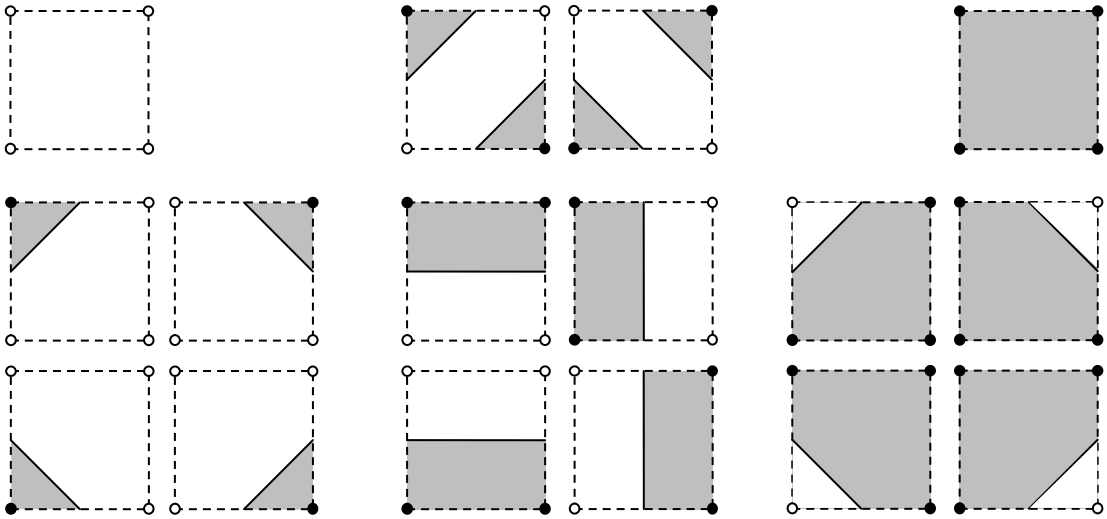

Figure 3.5. ***Example of all*** 16 ***possible ways how a*** 2***-dimensional isosurface can intersect a*** 2***-cube (square).***

Algorithm iterates through all possible labelings (intersections) and for each it executes:

a. Algorithm constructs the binary code χ, where each vertex can be assigned a bit 1, or bit 0, depending upon whether its value is greater or less than the equation value (isovalue) (***Fig. 3.6***). This code is unique for each labeling and will be used as an index key in a lookup table.

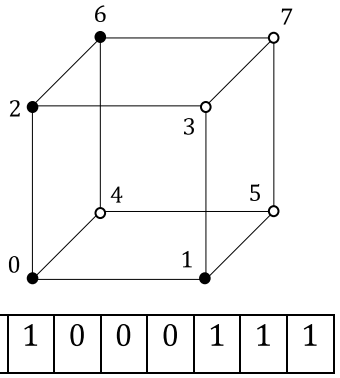

Figure 3.6. ***Example of the binary code for a single vertex labeling in*** $3D$***.*** *Here, vertices* $0, 1, 2, 6$ *are considered to be inside the surface, others - outside.*

b. Algorithm forms sets of points V^+ and V^-, where vertex's value is greater or less than the isovalue, respectively. Then algorithm constructs a set of points V^* which lie on the midpoints on the edges of hypercube between

points from V^+ and V^-. Let $W = V^* \cup V^+$ be a final set of points (***Fig. 3.7A***) [25].

c. Algorithm constructs canonically triangulated convex hull of W (***Fig. 3.7B***). The convex hull of W is a n-dimensional convex *n-polytope* lying in hypercube and approximating the set of points in the n-cube with positive isovalues [25]. Present implementation of the algorithm uses *Clarkson's Convex Hull* algorithm [29]. This algorithm uses fixed point arithmetic to avoid numerical inaccuracies in the computations. It also computes the convex hull, adding one vertex at a time, to ensure a canonical triangulation of the various cases. The incremental convex hull algorithm is not optimal, but provides a practical solution to a problem of generating consistent triangulation, moreover, it executes only for lookup table generation, which can be done only once.

d. Algorithm removes the $(n-1)$-dimensional facets of this convex n-polytope that lie on the boundary of the hypercube (***Fig. 3.7C***). This causes the removal of any facets, which share a vertex with the n-hypercube. Algorithm uses facets binary codes, calculated previously, for fast processing.

e. Remaining $(n-1)$-dimensional facets comprise the isosurface in the hypercube (***Fig. 3.7D***).

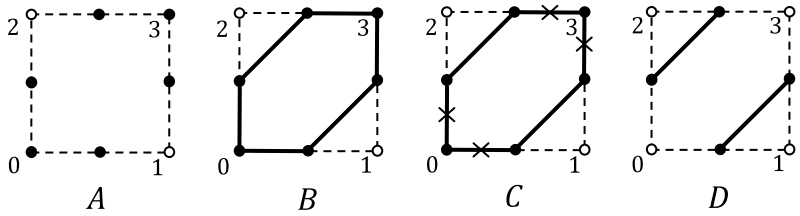

Figure 3.7. ***Extraction of simplices from an intersection points*.**

f. If resulting $(n-1)$-dimensional facets are not simplices (for example, in three dimensions there may exist two dimensional polygons with more than three vertices – imagine surface intersection angularly with a cube) then algorithm triangulates these facets so that the surface can be represented by a set of simplices. As stated before, Clarkson's Convex Hull algorithm [25, 29] adds points to the convex hull one at a time, so as

each point is added, the boundary of the new convex hull is constructed from the boundary of the previous one. The algorithm constructs not only the boundary of the convex hull but a triangulation of the boundary. Since the points and simplices are added incrementally, the resulting triangulation of each facet is a *canonical triangulation.* (*Let* $p_1, \dots, p_n$ *be points in convex position in* $\mathbb{R}^n$*. Triangulation* T *of* $convhull(p_1, \dots, p_n)$ *is called canonical if* $T - p_n$*, the simplicial complex* T *with all the simplices incident on* p_n *removed, is a canonical triangulation of* $convhull(p_1, \dots, p_{n-1})$*. A single simplex is a canonical triangulation [25]*).

g. Algorithm associates the resulting set of points with a code χ and writes the entry into the lookup table.

h. Obtained lookup table can be saved to hard drive and then algorithm can simply load it to avoid redundant recalculations.

5. Algorithm iterates through all n-dimensional hypercubes from a regular grid and determines how the algebraic equation intersects each n-hypercube (one-by-one). It uses the same method (as was used to build a lookup table) to determine which vertices are inside the surface and which are outside. According this information, algorithm constructs the binary code χ^* and search for it in lookup table. Lookup table returns a set of intersected edges and algorithm adjusts the simplices vertex locations by simple linear interpolation with real isovalues from algebraic equation.
6. At the end algorithm returns a set of simplices that form a complete surface, basically, algorithm constructs a triangulated $(n-1)$-manifold with a boundary in $\mathbb{R}^n$ [25]. For 3-dimensions that would be a set of triangles which can be visualized with OpenGL or DirectX® on a computer screen.

As a good test for this algorithm in three dimensions (to visually proof it correctness and applicability), we can visualize a well know *Sphere*, defined by following algebraic equation:

$$x^2 + y^2 + z^2 = 1$$

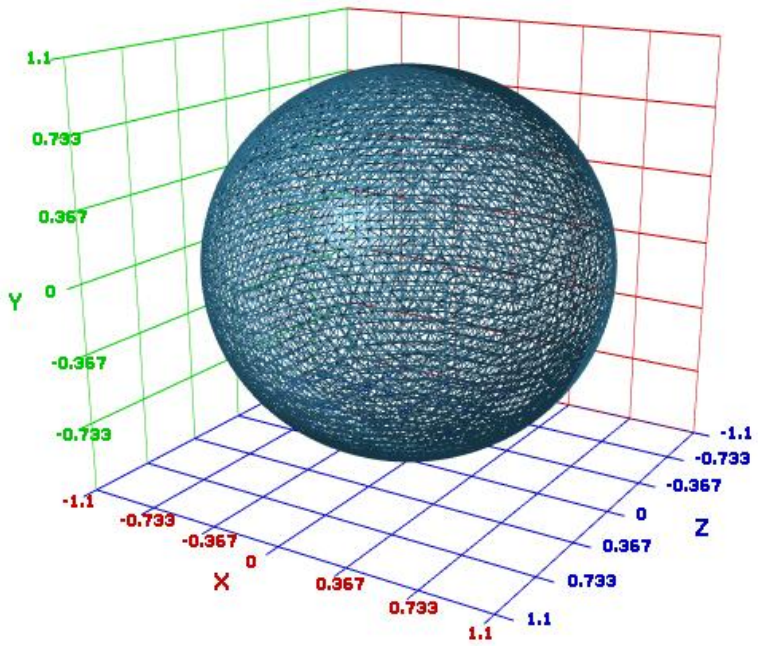

Figure 3.8. ***Sphere.*** *Defined as* $x^2 + y^2 + z^2 = 1$.

3.3. Parametric representation and superquadrics

To construct a parametric plot it is necessary to derive an explicit parametric representation of a manifold. Then by solving these parametric equations it is possible to obtain polygons which can be visualized. For example, consider a simple set of parametric equations for the circle in 2-dimensions

$$\begin{cases} x = r\cos t \\ y = r\sin t \end{cases}, \quad t \in (0, 2\pi).$$

By iteration through an independent parameter t, a set of points is calculated which exactly correlates with a circle. This principle can be used for any dimension.

To visualize a Calabi-Yau manifold immersed in $\mathbb{CP}^4$ described as homogeneous equation

$$z_1^5 + z_2^5 + z_3^5 + z_4^5 + z_5^5 = 0,$$

it is possible to slice it and, thus, reduce dimensionality (***Fig. 3.9***). We can produce a slice of this 6-manifold by assuming that some pair of complex inhomogeneous variables are constant. Let $\frac{z_3}{z_5}$ and $\frac{z_4}{z_5}$ be constant, so, after renormalization, equation

$$\boldsymbol{z_1^5 + z_2^5 = 1}$$

is produced, which is a 2-manifold slice embedded in real $4D$. We will use an idea of complex *superquadrics* to derive an explicit parametrization for this equation.

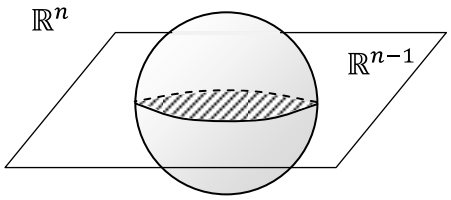

Figure 3.9. An e*xample of the cross-section (slice) of the n-dimensional sphere. Cross-section is $(n-1)$-dimensional.*

Superquadrics are a flexible family of deformable parametric curves and surfaces that are very useful for geometric modeling [15, 30, 31]. Their power lies in possibility to model large variety of shapes by adjusting a relatively few number of parameters. In two real dimensions ($\mathbb{R}^2$), the superquadric curves

$$\boldsymbol{|x_1|^n + |x_2|^n = 1}$$

interpolate between diamonds ($n = 1$), circles ($n = 2$) and squares ($n \to \infty$) for continuous n (***Fig. 3.10***).

Parametric representations of such superquadrics can be obtained by well known *Pythagorean trigonometric identity*

$$\cos^2 \alpha + \sin^2 \alpha = 1$$

and setting

$$a(\theta) = \cos\theta\,, \quad b(\theta) = \sin\theta\,, \quad 0 \le \theta < 2\pi$$

$$c(\theta) = (sign(a)|a|^{2/n},\ sign(b)|b|^{2/n})$$

Sign must be applied after power evaluation because of even powers, which forbid plotting negative values of functions. It is easy to show that this parametrization is valid, for example, for $n = 2$ equation is $c(\theta) = (\cos\theta\,, \sin\theta)$ which is a unit circle.

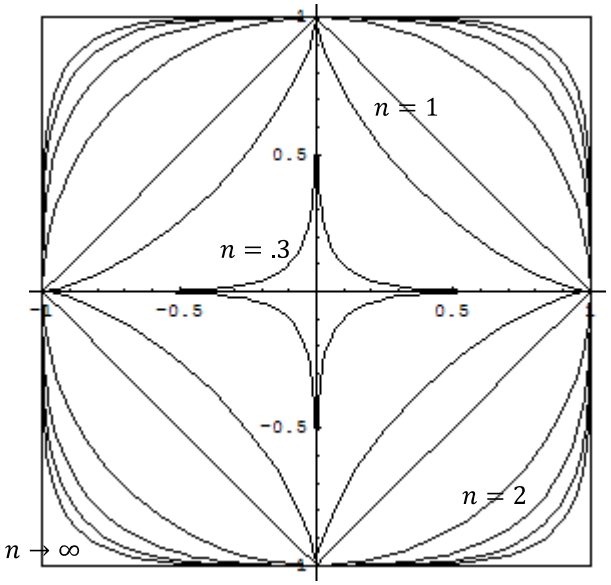

Figure 3.10. ***Plot of superquadric curves.***

Plot of parametric curve $c(\theta) = \left(sign(a)|a|^{2/n}, sign(b)|b|^{2/n}\right)$ *with different values of* n *- pinched diamond (*$n = .3$*), diamond (*$n = 1$*), circle (*$n = 2$*) and square* $(n \to \infty)$.

As an extension of quadric surfaces for $3\mathrm{D}$, four kinds of model can be distinguished: *supertoroid*, *superhyperboloid* with one or two sheets and *superellipsoid*. For instance, a superellipsoid is defined as the solution of the implicit algebraic equation:

$$\left(x^{\frac{2}{k}} + y^{\frac{2}{k}}\right)^{\frac{k}{l}} + z^{\frac{2}{l}} = 1$$

By using *Marching Cubes* method, it is possible to visualize these superellipsoids with different values l and k [30-32]:

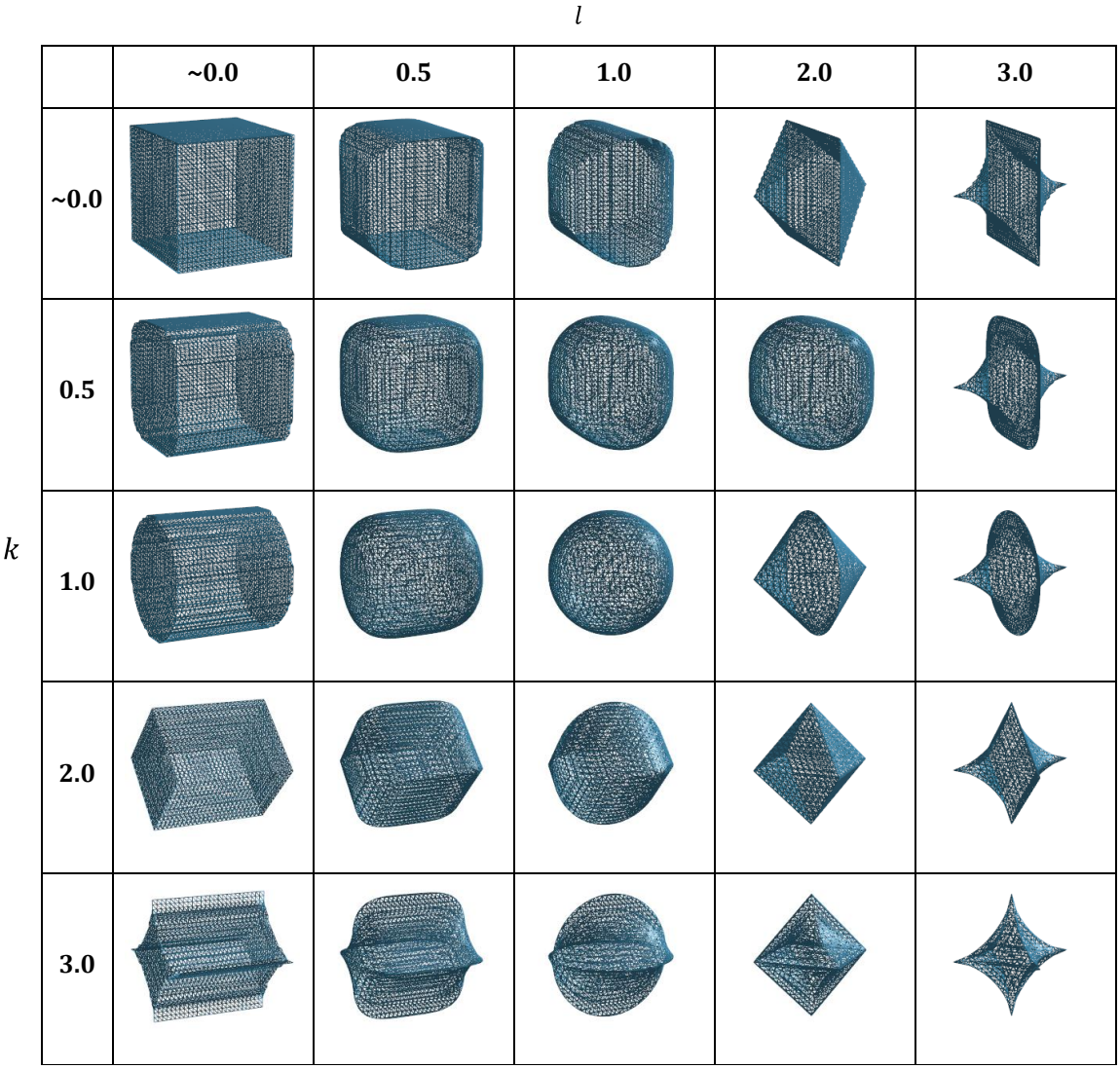

Figure 3.11. ***Plots of superellipsoids.***

Generally, it interpolate between parallelepiped ($l \to 0, k \to 0$), ellipsoid ($l = 1, k = 1$), cylinder ($l = 0, k = 1$) and so on.

Superellipsoid can be parametrized by *spherical product* of two 2D models (two superellipses). Let $a(\eta)$ be a superellipse defined on $-\pi/2 \leq \eta \leq \pi/2$ and $b(\omega)$ be second superellipse defined on $-\pi \leq \omega < \pi$, then by using of spherical a superellipsoid $c(\eta, \omega)$ will be obtained:

$$c(\eta,\omega) = a(\eta) \otimes b(\omega) = \begin{bmatrix} \cos^l \eta \\ \sin^l \eta \end{bmatrix} \otimes \begin{bmatrix} \cos^k \omega \\ \sin^k \omega \end{bmatrix}$$

$$= \begin{bmatrix} \cos^l \eta \cos^k \omega \\ \cos^l \eta \sin^k \omega \\ \sin^l \eta \end{bmatrix}, \quad \begin{matrix} -\pi/2 \leq \eta \leq \pi/2 \\ -\pi \leq \omega < \pi \end{matrix}$$

Implicit model have been used for visualization of superellipsoids, but this parametric model also can be used and it was proved itself as the easiest way [31].

Parametrization via Pythagorean trigonometric identity also can be used to visualize *complex superquadrics.* Homogeneous complexification of original equation $|x_1|^n + |x_2|^n = 1$ leads to surfaces defined as solutions of the homogeneous equation in $\mathbb{CP}^2$

$$z_1^n + z_2^n + z_3^n = 0$$

or, in general,

$$z_1^n + z_2^n = z_3^n$$

This equation can be represented locally in each of three regular $\mathbb{C}^n$ coordinate patches of $\mathbb{CP}^n$ where $z_1 \neq 0$, $z_2 \neq 0$ and $z_3 \neq 0$. Let $z_3 \neq 0$ so

$$\left(\frac{z_1}{z_3}\right)^n + \left(\frac{z_2}{z_3}\right)^n = 1$$

and, if $z_3 = 1$, final relation is obtained

$$\boldsymbol{z_1^n + z_2^n = 1.}$$

The hypothesis known as "*Fermat's Last Theorem*" reduces to the statement that with $z_3 = 1$ equation do not have real rational points for $\Re\mathrm{e}(z_1) > 0$, $\Re\mathrm{e}(z_2) > 0$ and $n > 2$ [33].

To visualize this complex algebraic equation the same parametric representation can be used as for real numbers, but at first it is necessary to define complex extension of sine and cosine. But first of all let's see what should be the definition of e^z for complex z. So $e^{x+iy} = e^x e^{iy}$ and last expression $e^{iy} = \cos y + i \sin y$, because of property of derivative $\left(e^{iy}\right)' = ie^{iy}$ - if $e^{iy} = a(y) + ib(y)$ then $a'(y) = -b(y)$ and $b'(y) = a(y)$, so $a(y) = \cos y$ and $b(y) = \sin y$ satisfy these relations. It is obvious that there is also $e^{-iy} = \cos y - i \sin y$ relation. For real y, if e^{iy} and e^{-iy} are added or subtracted, cosine

$$e^{iy} + e^{-iy} = \cos y + i \sin y + \cos y - i \sin y = 2 \cos y$$

$$\boldsymbol{\cos\theta = \frac{1}{2}\left(e^{i\theta} + e^{-i\theta}\right)}$$

and sine

$$e^{iy} - e^{-iy} = \cos y + i \sin y - \cos y + i \sin y = 2i \sin y$$

$$\boldsymbol{\sin\theta = \frac{1}{2i}\left(e^{i\theta} - e^{-i\theta}\right)}$$

can be obtained. By applying *principle of the permanence of functional relations*, complex extension of cosine can be derived for any complex number $z = (x + iy)$

$$\cos z = \frac{1}{2}\left(e^{iz} + e^{-iz}\right) = \frac{1}{2}\left(e^{i(x+iy)} + e^{-i(x+iy)}\right) =$$

$$= \frac{1}{2}\left(e^{ix}e^{-y} + e^{-ix}e^{y}\right) = \frac{1}{2}((\cos x + i\sin x)e^{-y} + (\cos x - i\sin x)e^{y}) =$$

$$= \cos x \cosh y - i \sin x \sinh y$$

and for sine

$$\sin z = \frac{1}{2}\left(e^{iz} - e^{-iz}\right) = \sin x \cosh y + i \cos x \sinh y$$

where $0 \leq x < 2\pi$ and $y \in \mathbb{R}$. So finally, necessary relation is found and complex Pythagorean identity can be expressed

$$u_1(x, y) = \cos(x + iy) = \frac{1}{2}\left(e^{i(x+iy)} + e^{-i(x+iy)}\right)$$

$$u_2(x, y) = \sin(x + iy) = \frac{1}{2}\left(e^{i(x+iy)} - e^{-i(x+iy)}\right)$$

$$(u_1)^2 + (u_2)^2 = 1$$

Previously, $sign(x)$ was used to find roots $\{1, -1\}$ for plotting negative values of real functions and now it must be extended to complex numbers too. We can achieve that by n-th *roots of unity*

$$r(k, n) = e^{\frac{2\pi k i}{n}}$$

where $k = 0, 1, 2, \ldots, n - 1$ and which, for example, for $n = 2$ will give $\{+1, -1\}$ and for $n = 4$ will give $\{+1, +i, -1, -i\}$ (***Fig. 3.12***).

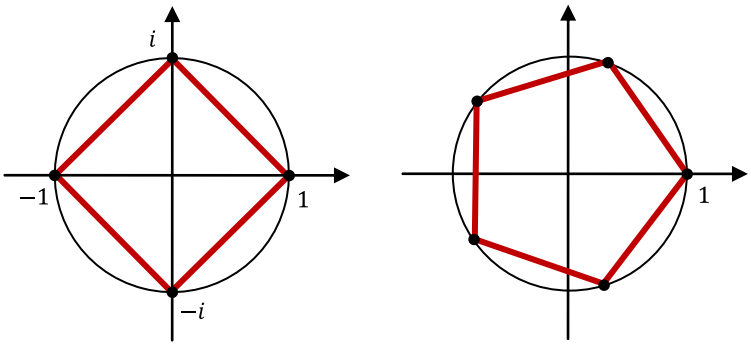

Figure 3.12. ***The 4^{th} and 5^{th} roots of unity.***

So equation $z_1^n + z_2^n = 1$ can be identically satisfied with following parametrization

$$W_x(x, y, k_1) = r(k_1, n)u_1(x, y)^{2/n}$$
$$W_y(x, y, k_2) = r(k_2, n)u_2(x, y)^{2/n}.$$

If we iterate through all possible values of $k_1$and k_2, then the equations produce a surface of one complex dimension in the $\mathbb{CP}^2$ (a surface of two real dimensions embedded in a real four dimensional space) for any n (***Fig. 4.8, 4.9, 4.10, 4.11***). Hence the surface floats in $4D$, to display it, the surface should be projected from $4D$ space to $3D$. It is possible to do it by combining the two imaginary components of W_x and W_y into a single three-dimensional coordinate z:

$$\begin{gathered} \boldsymbol{x = \mathfrak{Re}(W_x)} \\ \boldsymbol{y = \mathfrak{Re}(W_y)} \\ \boldsymbol{z = \cos\alpha \cdot \mathfrak{Im}(W_x) + \sin\alpha \cdot \mathfrak{Im}(W_y)} \end{gathered},$$

where $\alpha = \{0, 2\pi\}$. Although $k_1,\ k_2$ are in range $0, 1, 2, \dots, n-1$, so equation describes n^2 glued together *quadrilateral* (with four sides) patches in $\mathbb{C}^2$. Patches are related to each other by simple symmetry transformations and uncover intrinsic properties that numerical solutions would not be able to provide. By choosing different colors for every case of $(k_1,\ k_2)$ it is possible to color patches according to their complex phase (***Fig. 4.12, 4.13***). By varying α parameter or, by other words, an angle of projection, an animation can be rendered, which shows oscillating plot of different $4D \Rightarrow 3D$ projections.

3.4. Visualizer

This software was designed for visualization of different manifolds (defined as algebraic equations and in parametric form). It is written completely on C++ language in *Microsoft® Visual C++ 2005 IDE* [34] and it uses an *OpenGL®* [35] engine to render calculated data. It has a modified implementation of Marching Cubes algorithm, ability to calculate parametric plots, special classes structure to store calculated data in memory, embedded scripting language *Lua* [36] and several predefined surfaces for visualization. It has also some interactivity features like rotation and zooming with mouse control. Software consists from two parts: visualization *ActiveX* control (*m3dvisualizer*) and container (*m3dvisualizer*_test).

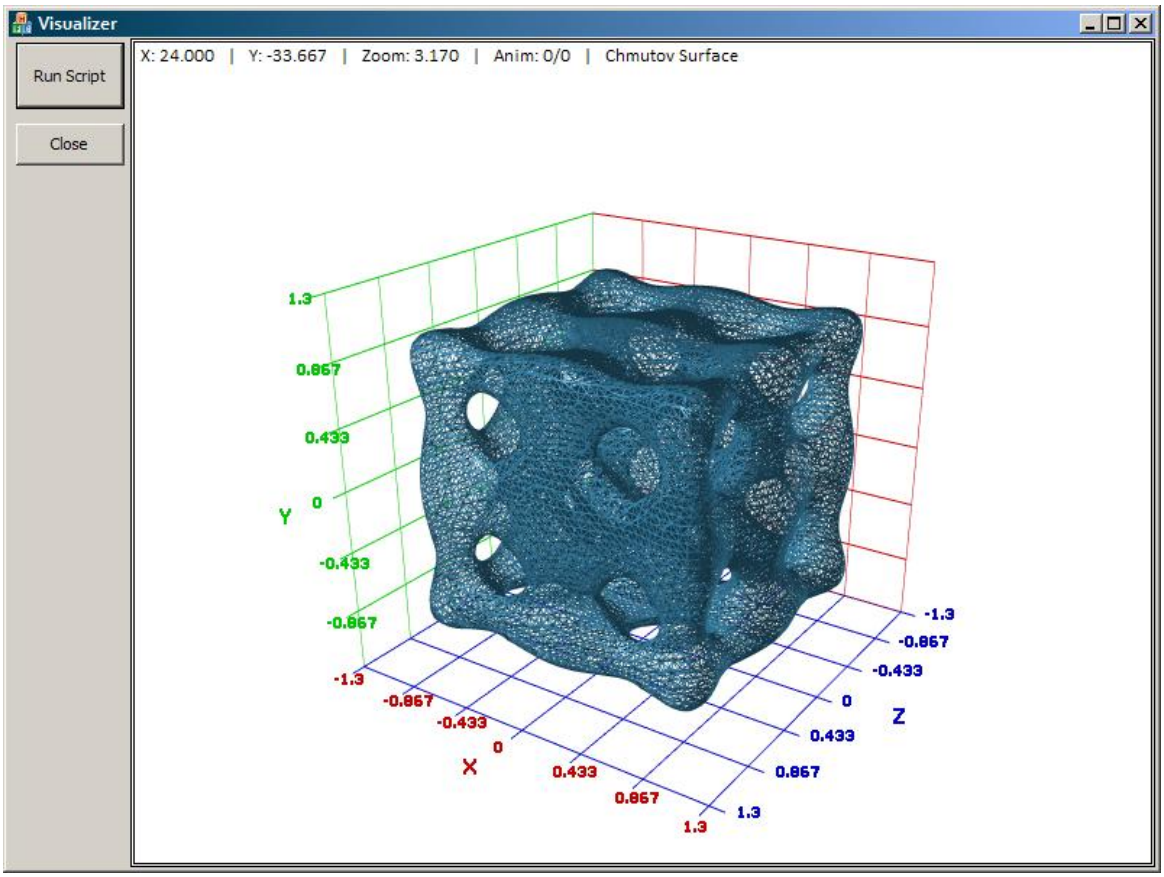

Figure 3.12. ***Software main screen.***

Software can load and execute simple scripts (Lua scripts). Each script can have different plot calculations and auxiliary methods that perform rotation, animation or zooming. Scripts were chosen because they provide very flexible way for application control. With scripts it is possible to specify desired plots and to easily apply custom

demonstration methods. All results for this thesis are calculated and rendered by this software.

These functions are available in scripts:

- **vis.AnimationNextStep**() – increments current animation step (usually used instead of `vis.AnimationSetStep(vis.AnimationGetStep() + 1)`);
- **vis.AnimationGetStep**() – returns current animation step;
- **vis.AnimationGetSize**() – returns maximum count of steps in current animation;
- **vis.AnimationSetStep**(*integer* ***step***) – sets current step in animation;
- **vis.CameraSetXY**(*integer* ***x***, *integer* ***y***) – sets current X and Y coordinates for a main camera position around the plot;
- **vis.CameraSetX**(*integer* ***x***) – sets current X coordinate for the camera position around the plot;
- **vis.CameraSetY**(*integer* ***y***) – sets current Y coordinate for the camera position around the plot;
- **vis.CameraSetZoom**(*integer* ***zoom***) – sets current zoom value for the camera;
- **vis.CameraGetX**() – returns current X coordinate of the camera position;
- **vis.CameraGetY**() – returns current Y coordinate of the camera position;
- **vis.SetTitle**(*string* ***title***) – sets a plot title;
- **vis.Invalidate**() – invalidates the plot;
- **vis.Wait**(*integer* ***milliseconds***) – waits in milliseconds (used for rotation or animation);
- **vis.MCEquation3D**(*string* ***name***, *integer* ***steps***, *boolean* ***isanimation***) – calculates a $3D$ plot with Marching Cubes algorithm (*name* can be "*kummerA*", "*kummerB*", "*chmutovA*", "*steiner_roman*", "*peninsula*", "*ellipsoid*");
- **vis.ParametricEquation**(*string* ***name***, *boolean* ***isanimation***) – calculates a parametric plot (*name* can be "*calabi*", "*mobius*", "*astell*");

The following sample sets camera position, adjust zoom, calculates plot with möbius parametric equation and performs rotation along Y axis of the plot:

```
function RotationY(max_cycles)
	cycles = 0;
	while cycles < max_cycles do
		vis.Invalidate();
		vis.Wait(40);
		yy = vis.CameraGetY() - 1.0;
		if yy < -360.0 then
			yy = 0.0;
			cycles = cycles + 1;
		end;
		vis.CameraSetY(yy);
	end;
end;

vis.CameraSetXY(21.0, -30.0);
vis.CameraSetZoom(3.17);
vis.SetTitle("Mobius Surface");
vis.ParametricEquation("mobius", false);
vis.Invalidate();
RotationY(100);
```

4. Results

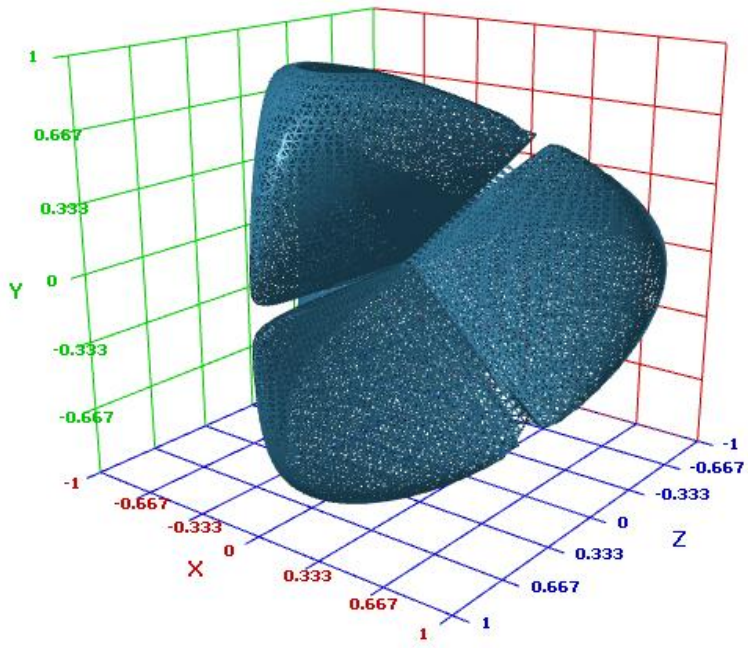

Figure 4.1. ***The Kummer surface.*** *Surface is defined with tetrahedral coordinates and with deformation parameter* $\mu = 1$ *(it is also known as Roman surface).*

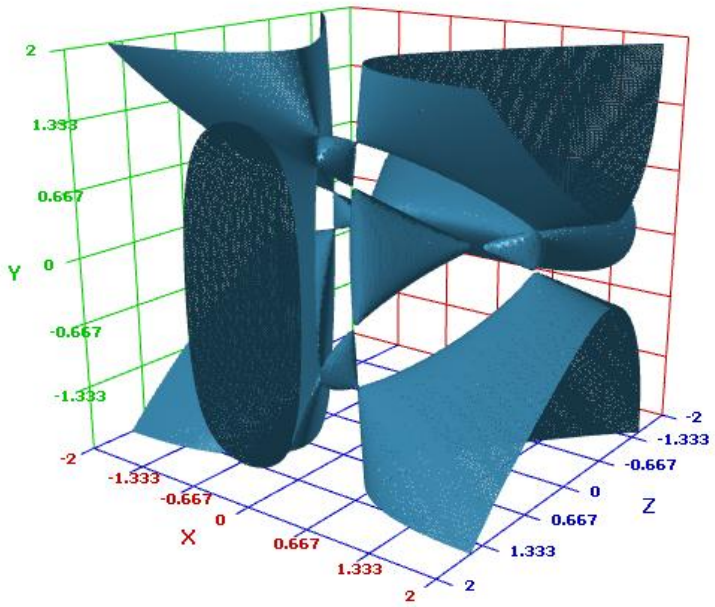

Figure 4.2. ***The Kummer surface.*** *Surface is defined with tetrahedral coordinates and with deformation parameter* $\mu = \sqrt{2}$*. Clearly* 16 *singular points are visible on this plot.*

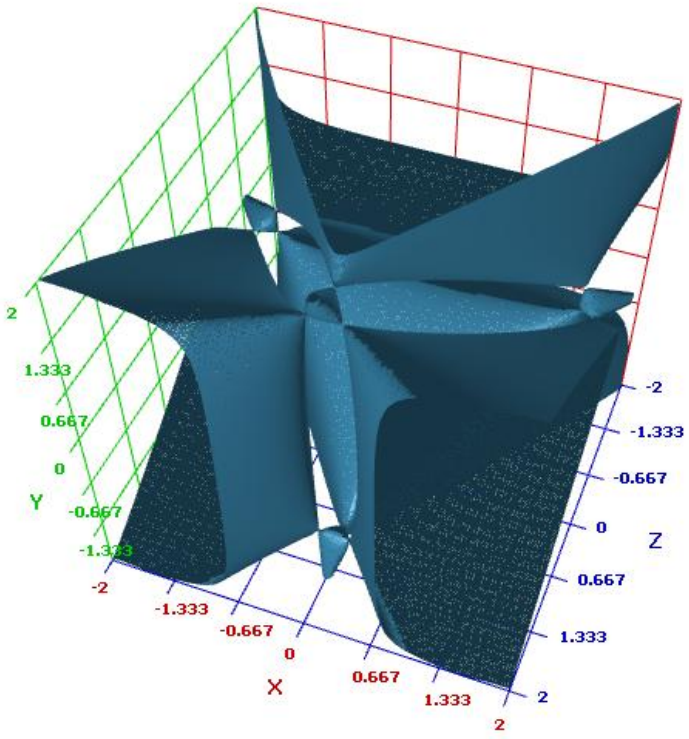

Figure 4.3. ***The Kummer surface.*** *Surface is defined with tetrahedral coordinates and with deformation parameter* $\mu = 2$.

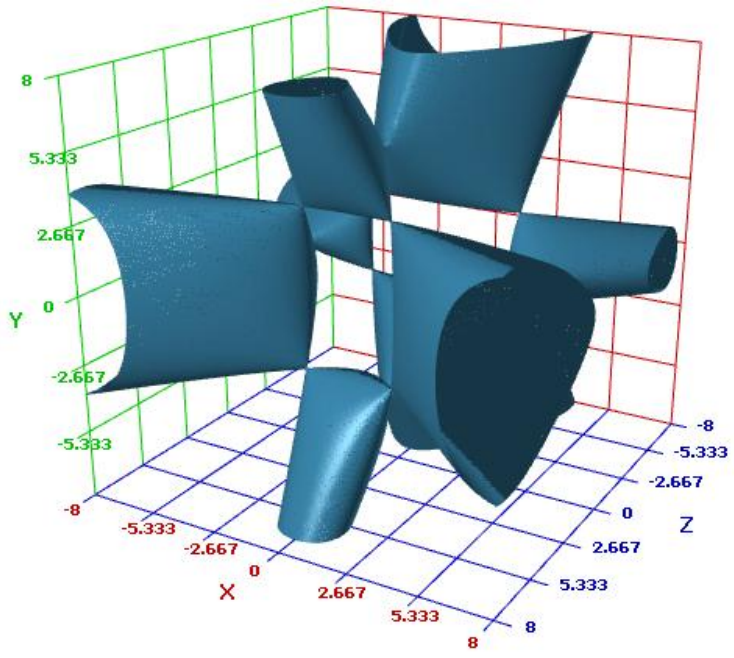

Figure 4.4. ***The Kummer surface.*** *Surface is defined with tetrahedral coordinates and with deformation parameter* $\mu = 5$.

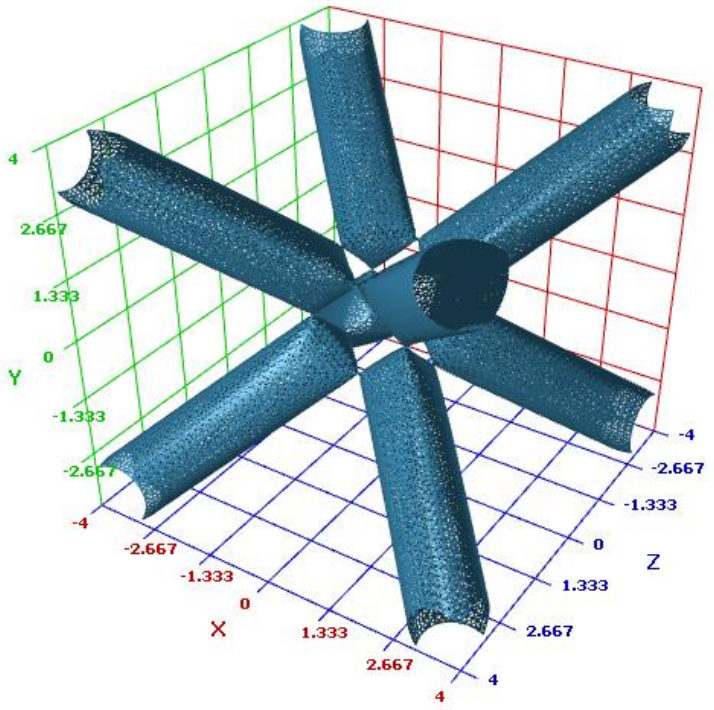

Figure 4.5. ***The Kummer surface.*** *Surface with singular points defined with equation*

$$x^4 + y^4 + z^4 - x^2 - y^2 - z^2 - x^2y^2 - x^2z^2 - y^2z^2 - 1 = 0.$$

The symmetry corresponding to the cube hidden in the central part and clearly visible on the plot.

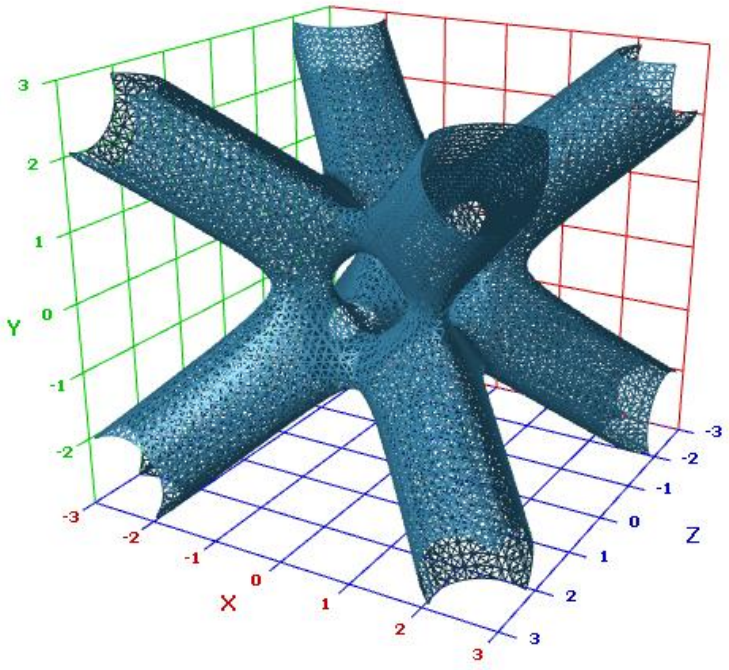

Figure 4.6. ***The non-singular Kummer surface (K3).*** *Surface defined with equation*

$$x^4 + y^4 + z^4 - x^2 - y^2 - z^2 - x^2y^2 - x^2z^2 - y^2z^2 - 1 = 0.3.$$

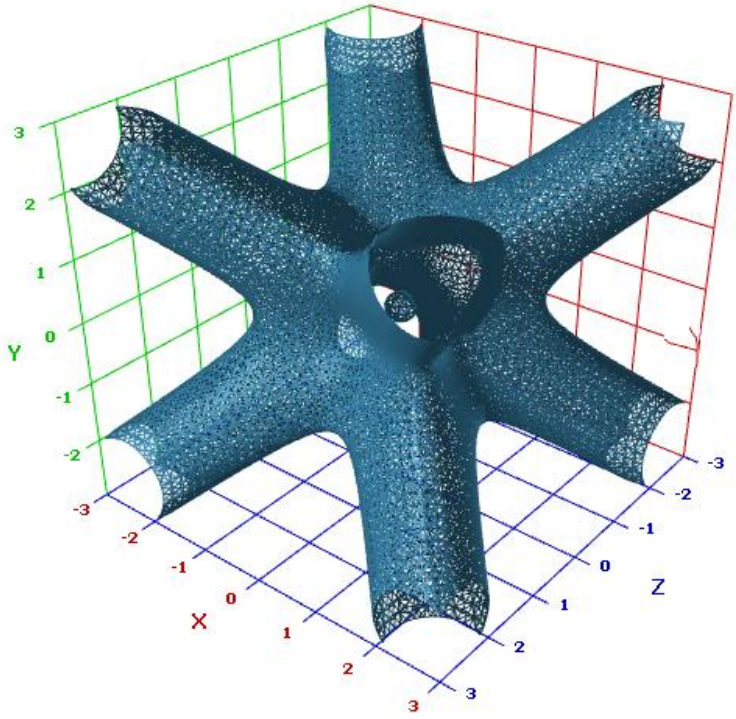

Figure 4.7. ***The non-singular Kummer surface*** $(K3)$. *Surface defined with equation*

$$x^4 + y^4 + z^4 - x^2 - y^2 - z^2 - x^2y^2 - x^2z^2 - y^2z^2 - 1 = 0.95.$$

A small sphere is visible inside.

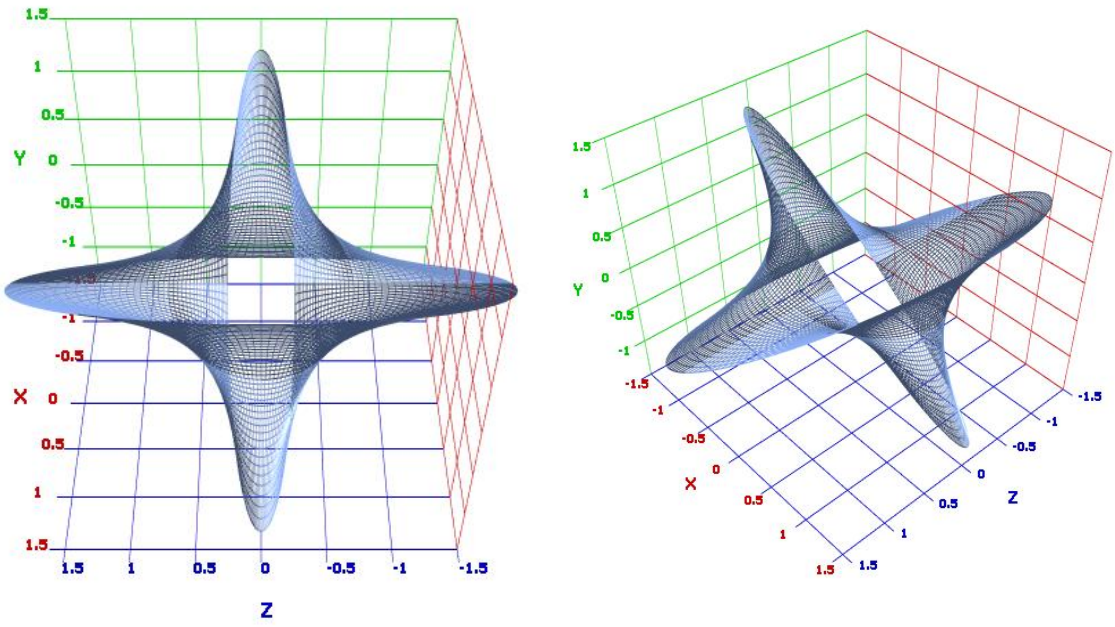

Figure 4.8. ***Parametric plot of complex equation*** $z_1^2 + z_2^2 = 0$. *The plot was rendered using complex superquadrics model.*

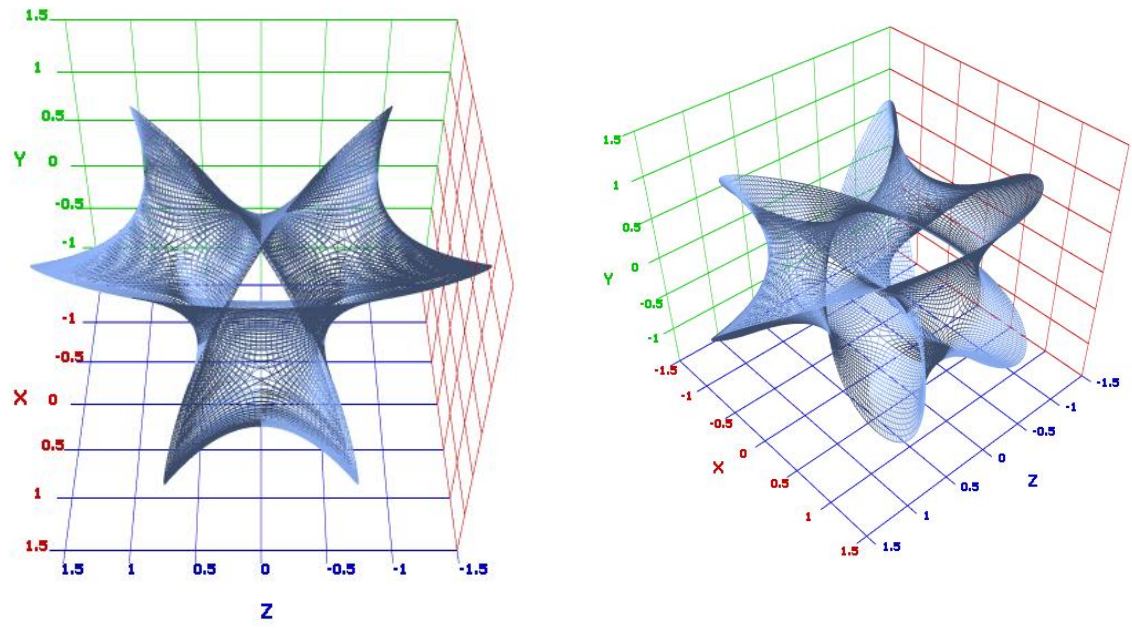

Figure 4.9. ***Parametric plot of complex equation*** $z_1^3 + z_2^3 = 0$. *The plot was rendered using complex superquadrics model.*

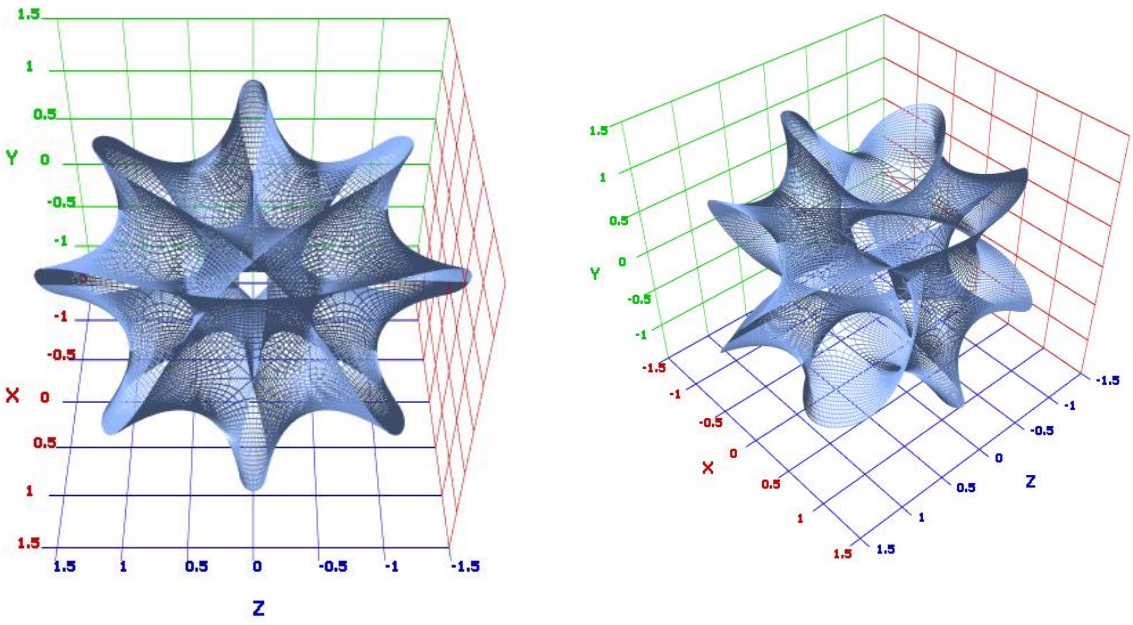

Figure 4.10. ***Parametric plot of complex equation*** $z_1^4 + z_2^4 = 0$. *The plot was rendered using complex superquadrics model.*

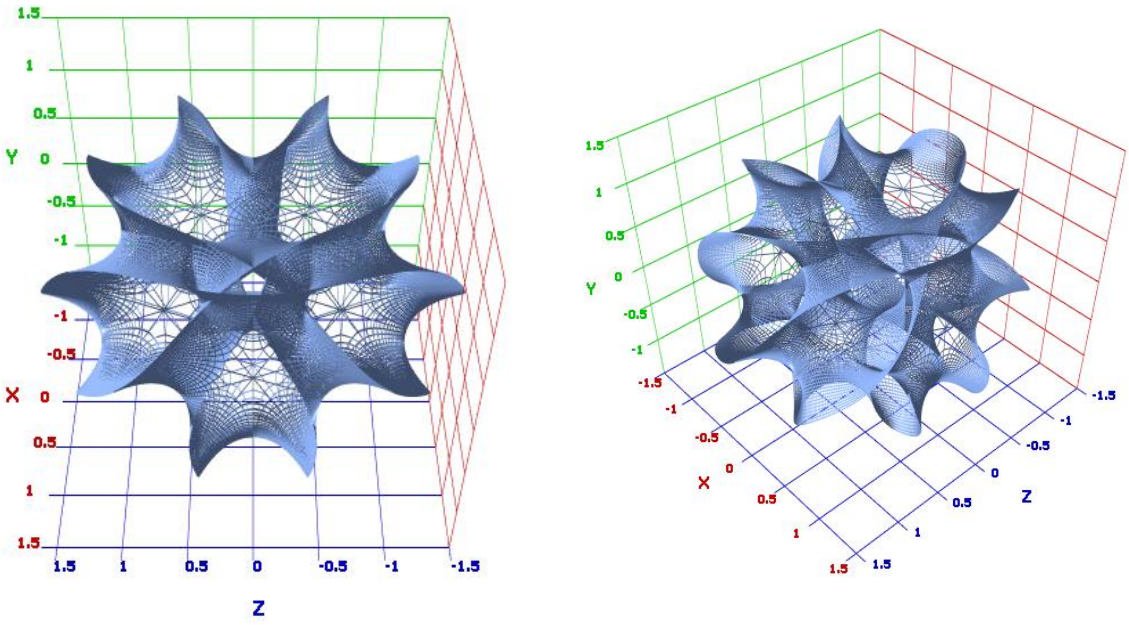

Figure 4.11. ***Parametric plot of complex equation*** $z_1^5 + z_2^5 = 0$. *The plot was rendered using complex superquadrics model. This is a two dimensional cross-section of a six-dimensional Calabi-Yau manifold* $z_1^5 + z_2^5 + z_3^5 + z_4^5 + z_5^5 = 0$. The shown surface is embedded in $4D$ and projected to $3D$.

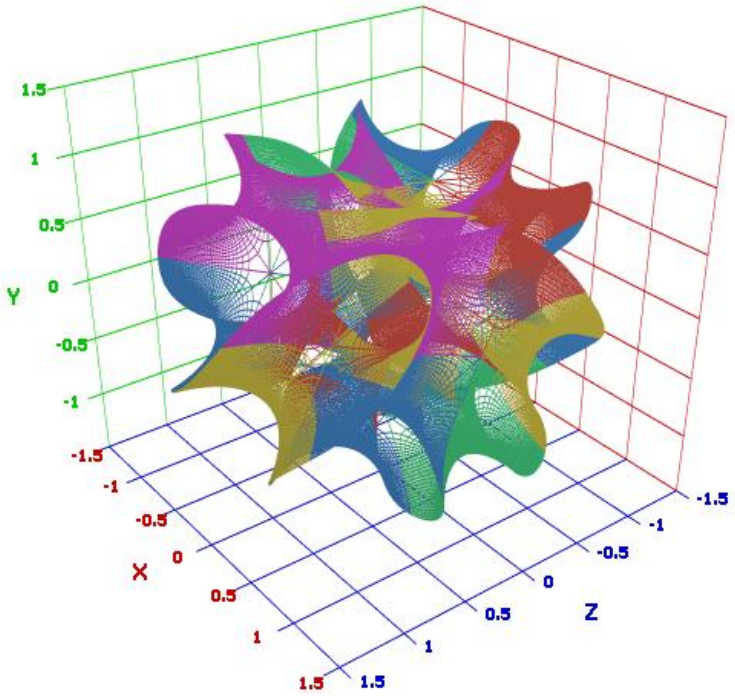

Figure 4.12. ***Parametric plot of complex equation*** $z_1^5 + z_2^5 = 0$. *Patches are colored according their complex phase.*

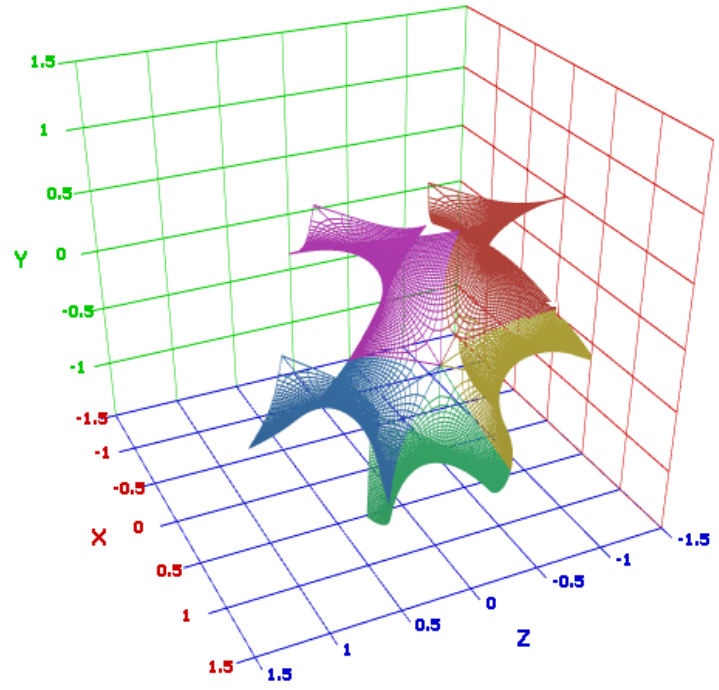

Figure 4.13. ***Parametric plot of five patches of complex equation*** $z_1^5 + z_2^5 = 0$. *Patches are colored according their complex phase. Clearly, five regions (patches) fanning out from a single point, are visible, which emphasizes the* ***quintic*** *nature of this surface.*

5. Summary

Within the bounds of this thesis an idea of extra dimensions was introduced and described - to give a reader some understanding how we came to this idea and why scientists really believe in them. Our cutting-edge physical theories (like superstring theories, supergravity, M-theory) in order to work and describe all, so far, observed physical phenomena, require additional degrees of freedom (extra dimensions). Since, we do not observe these extra dimensions (apparently, they are hidden in some way), one of the possibilities, which worth investigating, are compactifications. This method shrinks dimensions to a very small size (comparable to Planck length) and curls them up. Superstring theories compactify extra dimensions on a special kind of compact complex manifolds, called Calabi-Yau manifolds. They are special case of complex differential manifolds, which are compact, Kähler (endowed with closed Hermitian 2-form) and have $SU(n/2)$ holonomy. Precise mathematical definitions of such important structures are given in present thesis.

Then, we used two completely different visualization methods to render of some of the Calabi-Yau manifolds, like $K3$ surfaces and quintic hypersurfaces. An optimized Marching Cubes algorithm is used for construction of isosurfaces of algebraic equation in $3D$ and parametric representation via superquadrics is used for visualization of lower dimensional cross-sections of higher dimensional quintic hypersurfaces by projecting resulting 2-manifold from $4D$ to $3D$. Both methods are described in present thesis, are implemented in C++ language and plots are rendered with OpenGL engine in specially designed software called Visualizer. Our implementation is flexible and effective, because of highly optimized and specific algorithms. Also, it presents a possibility to render $4D$ plots, which are not available in common mathematical software (like Mathematica or MathCAD).

Since graphical information is the crucial type for human perception, such visualization methods are increase understanding and gaining intuition about these families of manifolds, and, thus, are very interesting to mathematicians and physicists. Generally, visualization helps to uncover some essential properties that are hidden within implicit equations of manifolds, and provides a tool for understanding their geometrical shapes.

6. Kokkuvõtte

Aegruumi kvantgeomeetriaga seotud komplekssete muutkondade visualiseerimine.

Selleks, et juhtivate füüsikateooriatega (superstringi, supergravitatsiooni ja M-teooria), saaks kirjeldada kõiki senini avastatud nähtusi, on vaja kasutatada lisa vabadusastmeid (lisadimensioone). Seni, kuni me ei saa jälgida neid varjatud lisadimensioone, oleks üheks lahenduseks kompaktifitseerimine. See meetod võimaldab lisadimensioone kokku tõmmata väikesteks (võrreldavad Planki pikkusega) ning kägardada kokku. Superstringi teooriates kompaktifitseeritakse lisadimensioone spetsiaalsete kompaktsete kompleksete Calabi-Yau muutkondade abil. Need on erijuht kompleksetest diferentseeruvatest kompaktsetest Kähleri muutkondadest, mis põhinevad kinnisel Hermitian 2-vormil ja omavad holonoomiarühma $SU(n/2)$. Nende oluliste struktuuride täpsed kirjeldused on esitatud antud töös.

Antud väitekirjas piirdume visualiseerimisel Calabi-Yau kahe muutkonnaga: $K3$ pinnad ja viienda astme hüperpinnad (*quintic hypersurface*). $K3$ pindade visualiseerimiseks kasutame enda poolt oluliselt optimiseeritud Marching Cubes algoritmi, mille abil on konstrueeritud algebraliste võrrandite tasemepinnad $3D$-s. Viienda astme hüperpindade visualiseerimiseks on kasustatud superkvadrikuid, millega on võimalik näidata kõrgedimensionaalsete viienda astme hüperpindade lõikeid ruumis madalama dimensionaalsusega: 2-muutkond projekteeritakse neljadimensionaalsest kolmedimensionaalsse ruumi. Antud töös kirjeldatakse mõlemat meetodit, rakendatakse C++ keeles ja esitatakse pindade graafikud, mis on tehtud spetsiaalselt selle probleemi lahendamiseks loodud tarkvaraga Visualizer, koos OpenGL mootoriga. Rakendatavus on paindlik ja efektiivne tänu olulisel määral optimiseeritud ja spetsiifilistele algoritmidele. Samuti on võimalik algoritmi kasutada neljadimensionaalsete graafikute näitamiseks. Antud võimalus puudub teistes tundud tarkvarades (Mathematica ja MathCAD).

Käesolev töö võiks pakkuda huvi matemaatikutele ja füüsikutele, sest töös kasutatavad visualiseerimismeetodid täiendavad teadmisi ja ettekujutust nendest muutkondadest. Visualiseerimine aitab esile tuua muutkondade varjatud põhiomadusi ja annab vahendi nende geomeetrilise kuju mõistmiseks.

References

1. Bryanton, R., *Imagining the Tenth Dimension*. 2006: Talking Dog Studios. 216.

2. Greene, B., *The Elegant Universe: Superstrings, Hidden Dimensions, and the Quest for the Ultimate Theory*. 1st ed. 1999, New York: W. W. Norton. xiii, 448 p.

3. Greene, B., *The Fabric of the Cosmos: Space, Time, and the Texture of Reality*. 1st ed. 2004, New York: A.A. Knopf. xii, 569 p.

4. Penrose, R., *The Road to Reality: a Complete Guide to the Laws of the Universe*. 1st American ed. 2005, New York: A.A. Knopf. xxviii, 1099 p.

5. Kaluza, T., *On the Problem of Unity in Physics*. 1983, Knudsen.

6. M. J. Duff, B.E.N., C. N. Pope, *Kaluza-Klein Supergravity*. 1985: CERN, Geneva.

7. Greene, B., *String Theory on Calabi-Yau Manifolds*, in *Lectures given at Theoretical Advanced Study Institute in Elementary Particle Physics (TASI 96): Fields, Strings, and Duality, Boulder*. 1997. p. 150.

8. Witten, E., *Universe on a String*. 2002: www.astronomy.com. p. 3.

9. Witten, E., *Reflections on the Fate of Spacetime*. 1996: American Institute of Physics.

10. Witten, E., *Duality, Spacetime and Quantum Mechanics*. 1998: Institute for Advanced Study (Princenton).

11. Zwiebach, B., *A First Course in String Theory*. 2004, New York: Cambridge University Press. xx, 558 p.

12. Randall, L., *Warped passages : unraveling the mysteries of the Universe's hidden dimensions*. 1st ed. 2005, New York: Ecco. xii, 499 p.

13. Susskind, L., *Cosmic landscape : string theory and the illusion of intelligent design*. 1st ed. 2005, New York: Little, Brown and Co. xii, 403 p.

14. Hitchin, N., *Generalized Calabi-Yau Manifolds*. 2006: Oxford.

15. Hanson, A.J., *A Construction for Computer Visualization of Certain Complex Curves.* Notices of the Amer. Math. Soc, 1994. **41**(9): p. 1156-1163.

16. Wells, R.O., *Differential Analysis on Complex Manifolds*. 1973: Prentice-Hall Inc.

17. Chern, S.-S., *Complex Manifolds without Potential Theory: with an Appendix on the Geometry of Characteristic Classes*. 2d ed. Universitext. 1979, New York: Springer-Verlag. 152 p.

18. Candelas, P., *Lectures on Complex Manifolds*. 1987: Theory Group, Department of Physics, The University of Texas.

19. Hübsch, T., *Calabi-Yau Manifolds. A Bestiary for Physicists*. 1992: World Scientific Publishing. 362.

20. Smith, J., *Introduction to K3 Surfaces (Part 2).* 2005.

21. Kallosh, R., *Towards String Cosmology.* Progress of Theoretical Physics, 2006(163).

22. Kallosh, R., *Fixing All Moduli for M-Theory on K3xK3*. 2005: Superstring Phenomenology 2005.

23. Hudson, R.W.H.T., *Kummer's Quartic surface*. 1990: Cambridge Univesity Press.

24. Bhaniramka, P., *Isosurfacing in Higher Dimensions*, R.C. Rephael Wegner, Editor. 2000.

25. Bhaniramka, P., *Isosurface Construction In Any Dimension Using Convex Hulls*, R.C. R. Wegner, Editor. 2003.

26. Lorensen, W.E., *Marching Cubes: A High Resolution 3D Surface Construction Algorithm*, H.E. Cline, Editor. 1987, Computer Graphics: ACM.

27. Roberts, J.C., *Piecewise Linear Hypersurfaces using the Marching Cubes Algorithm*, S. Hill, Editor. 2006.

28. Weigle, C., *Complex-Valued Contour Meshing*, D.C. Banks, Editor. 1996, IEEE.

29. *Clarkson Convex Hull Algorithm*. [cited; Available from: http://cm.bell-labs.com/who/clarkson/index.html.

30. Bourke, P., *Superellipse and Superellipsoid, A Geometric Primitive for Computer Aided Design*. 1990.

31. Jaklic, A., *Segmentation and Recovery of Superquadrics*, ed. A. Leonardis. Vol. 20. 2000: Springer. 267.

32. Chevalier, L., *Segmentation and superquadric modeling of 3D Objects*, A.B. Fabrice Jaillet, Editor. 2003, Journal of WSCG.

33. Hanson, A.J., *Techniques for Visualizing Fermat's Last Theorem: A Case Study*, B.C.K. P.A.Heng, Editor. 1990, IEEE.

34. *Microsoft Visual C++ 2005*. [cited; Available from: http://msdn2.microsoft.com/en-us/vstudio.

35. *OpenGL - The Industry's Foundation for High Performance Graphics*. [cited; Available from: http://www.opengl.org/.

36. *The Programming Language Lua*. [cited; Available from: http://www.lua.org/.